2019

Characterization of the Red Complex Bacterial Biofilm

Alena Pratasouskaya
prat2880@mylaurier.ca

Characterization of the Red Complex Bacterial Biofilm

by

Alena Pratasouskaya

Bachelor of Science Biochemistry and Biotechnology degree, Wilfrid Laurier University, 2017

THESIS

Submitted to the Department of Chemistry and Biochemistry

In partial fulfilment of the requirements for

Master of Science in Chemistry

Wilfrid Laurier University

Abstract

Commonly associated with severe inflammation and destruction of the tooth supporting tissue is bacterial consortia *Treponema denticola, Tannerella forsythia, and Porphyromonas gingivalis*, collectively referred to as the red complex. The red complex uses the common bacterial strategy of producing and imbedding itself in extracellular polymeric substance, which contributes to the recalcitrance of periodontitis and was therefore of interest in this study. The red complex static cultures were grown in combination with different chemicals in order to establish what changes accompany these chemical challenges. This research established that extracellular polymeric substance carbohydrate yields increased with time. Interestingly, carbohydrate composition via gas chromatography - mass spectrometry analysis detected increase of mannose and galactose in the samples challenged with tetracycline, and decrease of these sugars in cultures challenged with hydrogen peroxide. Understanding the molecular features that contribute to biofilm formation in the red complex will offer unique insights into how bacteria communicate and thrive under various conditions and may provide strategies to mitigate periodontal disease. The results of this study have the potential to identify new mechanisms of biofilm establishment and persistence. These insights may ultimately lead to new methods to disrupt biofilm formation, which could benefit diverse sectors ranging from natural resource extraction, water resource management, and health.

Acknowledgements

I would like to express my sincere gratitude to my Professor Dr. Geoff Horsman for his immense knowledge, support, encouragement and guidance. I also would like to say thank you to my committee members Dr. Michael Suits, Dr. Joel Weadge, and Dr. Robin Slawson. Your input and revisions were very much appreciated.

A separate thank you to Dr. Slawson for providing me with the opportunity to work in her anaerobic chamber. Without this equipment this research would not be possible.

A special thank you goes to Dr. Mario Monteiro for giving the opportunity to work in his lab under supervision of my friend Jennifer Crha. Thank you to Dr. Monteiro for valuable experience in carbohydrate derivatization and mass-spectrometry analysis.

Thank you to Jennifer Crha for helping me throughout my mass-spec carbohydrate analysis, for all your hours spent teaching me the procedure and analysis.

I am expressing my sincere gratitude to Wilfrid Laurier University for providing the environment facilitating to success as well as providing financial support to a researcher in the form of scholarships and tuition bursaries.

Thank you to GlycoNet for funding this project and providing me with the opportunity for collaboration and personal growth.

Table of Contents

List of Abbreviations

QS	Quorum sensing
EPS	Extracellular polymeric substances
LPS	Lipopolysaccharide
PrtP	Propyl-phenylalanine specific protease
ECM	Extracellular matrix
PS	Polysaccharides
GT	Glycosyltransferase
PCP	Polysaccharide co-polymerase
CPS	Capsular polysaccharides
Kdo	2-keto-3-deoxyoctulosonic acid
DP	Degree of polymerization
Glc	Glucose
Gal	Galactose
GlcNAc	N-acetylglucosamine
GalNAc	N-acetylgalactosamine
Man	Mannose
DNA	Deoxyribonucleic acid
RNA	Ribonucleic acid
ATCC	American Type Culture Collection
OBGM	Oral Bacterium Growth Medium

OD	Optical density
SDS-PAGE	Sodium dodecyl sulfate – polyacrylamide gel electrophoresis
PS	Polysaccharides
AA	Alditol acetate
AcOH	Acetic acid
Ac_2O	Acetic anhydride
GC-MS	Gas Chromatography and Mass Spectroscopy
DCM	Dichloromethane
PMAA	Partially methylated alditol acetate
DMSO	Dimethyl sulfoxide
BSA	Bovine Serum Albumin
RT	Retention times
RRT	Relative Retention times
QS	Quorum sensing molecule

List of Tables

List of Figures

Introduction

The Complexity of Bacterial Community

After first observation of bacteria by Van Leeuwenhoek in 1683[1] numerous studies show the complexity of bacterial communities. Misconception to think that bacteria spend their entire lives in a "planktonic state" as individual free-floating organisms. Microorganisms have a tendency to form sedentary communities on different surfaces[2] and imbed the community in self-produced extracellular matrix (ECM) for survival. Microbial cells and ECM together are called biofilm. Production of ECM is very complex since it depends on production and secretion of extracellular material by cells. However, the high energetic cost is presumably justified by the beneficial properties of the biofilm.

The biofilm can be compared to a city, where many living cells are distributed and organised in homes, such as the ECM. Therefore, ECM molecules facilitate formation of the biofilm as a whole and can be compared to the buildings of the city. ECM determines the architecture of the biofilm by shaping and filling the spaces between the cells and providing the mechanical support[3]. The biggest percentage of the ECM matrix is water (up to 97%), but also contains different components, such as proteins, extracellular deoxyribonucleic acid (eDNA), polysaccharides, lipids[4]. The structure of ECM contains porous and channel-like arrangement in order to facilitate liquid transportation and communication between cells including horizontal gene transfer[5].

One of the essential features of a biofilm is its ability to be remodelled. Biofilm is dynamic and continuously changes with its environment[6]. Participating microorganisms have advantages for survival including, for example, increased resistance to host defences and antimicrobial agents such as chlorhexidine[7]. Chlorhexidine had effect only on outer layer of 48-hour dental biofilm or newly formed one in the study conducted by Zaura-Arite *et.al.* The vitality was observed with increase age of the biofilm. Living in the community broadens habitat range and enhances pathogenicity[8], for example, through degradation potential of the biofilm by producing extracellular vesicles packed with enzymes[9], which also facilitate dispersal and colonization on a surface. Other contributions to community survival include use of eDNA, cationized exopolysaccharides for crosslinking and structural integrity of the matrix[10], production of curli proteins, which are a type of amyloid fiber that, in combination with cellulose, contribute to tolerance of biofilm to desiccation.[10] Some bacteria also contribute to electron transport via production of pili that are used as nanowires and proteinaceous filaments[11]. The communal diversity exists to provide complimentary metabolic processes to sustain and support beneficial species while excluding many other species that are either not capable of growing in this environment or inhibited by bacteriocins or bacteriocin-like substances[12]. The host diet and lifestyle can influence the assortment of the bacteria by shifting the proportions of some species[13]. For example, increased consumption of sugar leads to increased populations of lactobacilli and diminishment of *Streptococcus oralis* in an oral biofilm community. These changes decrease the environmental pH due to fermentation of sugars to lactic acid,[13] which

causes erosion of the outermost layer of tooth enamel in a process called demineralization[14]. Cells in a biofilm are able to adjust to new local conditions by coordinating life cycles, which includes expression of new genes and production of new proteins[15]. Biofilm is not a simple waste excreted from the cells; it is a highly organized, heterogeneous matrix that contributes to bacterial survival in challenging conditions.

From Plaque to Periodontal Disease

Plaque biofilm represents one bacterial community of particular importance to human health[5]. Dental plaque harbours over 600 bacterial species[16,17]. According to the National Institute of Dental and Craniofacial Research, dental caries is the most prevalent infectious condition worldwide caused by demineralization of enamel and bacterial communities that accumulate in plaque[18]. This untreated condition can lead to periodontal disease, which is inflammation and destruction of teeth supporting tissue such as the periodontal ligament, alveolar bone and soft tissues[19]. According to statistics of the American Academy of Periodontology, as of 2012 every other American adult over the age of 30 has periodontal disease at different progression[18]. Periodontitis needs to be treated in order to prevent tooth loss as well as other serious diseases associated with periodontitis, such as cardiovascular disease[20], diabetes[21], cancer[22], and other inflammatory conditions[23]. The mechanism of bacterial colonization and aggregation leading to dysbiosis and to dental diseases is poorly understood. However, it is well known that microbial communities attached to the surface and embedded in self-produced extracellular polymeric substances are sheltered from environmental stress and provide perfect

conditions for a greater diversity of microorganisms[24,25,26]. Such diversity is required for maintenance of homeostasis within a microbial community[27]. For example, metabolism end product of oxygen-consuming species provide a good environment for obligate anaerobes[28].

Red Complex

Studies of bacterial communities of subgingival dental plaque reveal over 500 participating bacterial species[17]. Some of them are present in healthy sites of subgingival culture, while others are strongly associated with periodontal disease[29,30]. Periodontitis is a severe inflammation and destruction of the tooth supporting tissue associated with bacteria. Socransky *et al*.[1] examined > 13 000 plaque samples and inventoried bacterial species into five major color-coded microbial complexes based on the subgingival depth occurrence of species and relationship among them. In severe cases of periodontitis, prevalence of bacteria *Treponema denticola (Tde), Tannerella forsythia (Tfo)* (previously named *Bacteroides forsythus),* and *Porphyromonas gingivalis (Pgi)* was observed[31,28]. This consortium was color-coded red, therefore termed the Red Complex, and has been shown to be associated with chronic periodontitis[29,30,31,] Red complex species are all Gram-negative anaerobes with apparent co-dependency. For example, *T. denticola* is not found at the site of infection without the presence of *P. gingivalis*[32] and *P. gingivalis* was always accompanied by *T. forsythia.* These findings suggest that progression to chronic periodontitis requires all three bacterial species[33].

Porphyromonas gingivalis

P. gingivalis was discovered in the 1980's and investigated for pathogenicity and role in progression of periodontal disease[34]. The preferred environment for these Gram-negative, non-motile, asaccharolytic anaerobes is the subgingival groove of the oral cavity[35]. *Porphyromonas gingivalis* secrete different virulence factors, such as fimbriae, different proteolytic enzymes, capsule, and others.

Different virulence factors are important for reproduction of the bacterial species in the host. Fimbriae are thin protein structures found on the outer membrane of bacterial cells, including *P. gingivalis*, which participate in initial invasion through adhesion to the host cell outer membrane[36]. Fimbrillin is a structural component of fimbriae encoded by the *fimA* gene with a molecular mass of 43 kDa[31]. Initial attachment of *P. gingivalis* to mucosal and tooth surfaces as well as bacterial co-aggregation is facilitated by fimbrillin, which binds to proline-rich proteins in human saliva. Absence of *fimA* gene resulted in inability of *P. gingivalis* to attach and invade epithelial cells of the host[37]. Some genes involved in fimbriae formation were investigated for involvement in production of biofilm. Genes *fimR and fimS* of *P. gingivalis* were upregulated during biofilm formation[38]. These genes are important in monitoring the specific signals from the environment.

Another virulence factor of *P. gingivalis* is protease enzymes that facilitate bacterial thriving in the host. Serine proteases and cysteine proteases are called gingipains. Gingipain R cleaves polypeptide at arginine amino acid close to C-terminus, while gingipain K cleaves at lysine. The role of these enzymes is to degrade extracellular matrix proteins collagen, which is a host structural protein,

and fibronectin that plays role in blood clotting [39]. The supply of the blood at the site of the infection brings heme proteins that are decomposed by gingipains[39]. This process guarantees the supply of iron needed for *P. gingivalis* growth since it cannot ferment sugars and needs iron for development[40]. Due to acquisition of hemoglobin from the medium to furnish a cell surface hemin layer *P. gingivalis* colonies are black in color[41]. Gingipains also impair the host defence mechanism through destruction of immunoglobulin[42]. Increased activity of serine protease leads to destruction of the tissue at the infected site[42]. The degraded host proteins supply amino acids that *P. gingivalis* uses for growth and construction of its own proteins.[42]

Capsule presents a virulence factor that facilitates the survival of *P. gingivalis* due to its presence on the outer membrane. Lipopolysaccharide (LPS), glucosamine, uric acid, and glucose are components of capsule and play important roles in protecting bacteria from phagocytosis. The LPS activates macrophages using Toll-like receptor, but previously produced ECM protects the bacteria from phagocytosis[43]. Activated macrophages start the cascade leading to the destruction of the surrounding tooth tissue and the alveolar bone. Produced by macrophage cytokines activate neutrophils, which play a role in inflammation development[43]. Since the immune response is not efficient at killing bacteria embedded in biofilm, the chronic response causes more damage to the host tissue and ultimately leads to tooth loss.

Treponema denticola

Treponema denticola is a motile, Gram-negative obligate anaerobic spirochete bacterium. Several studies have shown a relationship between the

presence of *T. denticola* and its role in transitioning healthy tissues to periodontitis due to many virulence factors produced by this species. For example, metabolically produced hydrogen sulfide (H_2S) is cytotoxic to fibroblasts and epithelial cells of host[44]. Besides providing a suitable environment for other bacteria of the red complex *T. denticola* produces growth enhancing fatty acids and promotes the growth of other species. Yamada and colleagues have demonstrated mutualistic help during biofilm formation between *T. denticola* and *P. gingivalis*[45]. A symbiotic relationship for utilization of nutrients among these microbes was also demonstrated[46]. Unlike other bacteria *T. denticola* does not have lipopolysaccharides (LPS) and, therefore, does not produce endotoxin[47]. Instead these bacteria produce lipoproteins that trigger inflammation in host tissue[48].

Many *T. denticola* genes involved in biofilm formation were identified and studied. The *flgE* gene encodes flagella hook protein, which increases motility of bacteria facilitating host tissue invasion and formation of biofilm matrix due to increase length of the flagella[49]. The *msp* gene is responsible for production of a major surface protein involved in cytotoxic effect towards epithelial cells due to its pore-forming abilities and adhesion effect due to association with chymotrypsin-like protease. Supply of nutrients from damaged host cells and ability to adhere facilitate successful biofilm formation[47]. *T. denticola* lacking cytoplasmic filament protein, gene *cfpA,* is unable to form biofilm specifically with *P. gingivalis* and has reduced ability to form biofilm on its own[32]. Finally, deletion of propyl-phenylalanine specific protease (PrtP) showed decrease of *T. denticola* ability to survive in biofilm due to reduction of expression other sheath proteins[50].

Tannerella forsythia

Tannerella forsythia is a Gram-negative, anaerobic bacterium previously called *Bacteroides forsythus.* The investigation of these species was delayed due to difficulty in finding appropriate growth conditions[33]. *T. forsythia* is not capable of breaking down sugars and, therefore, obtains energy for growth by scavenging peptides, which are broken down by cysteine-like and trypsin-like proteases PrtH[51]. These proteins also have the ability to arrest periodontal tissue cells in the G2 phase, reduce adherence, affect the immune system, and induce production of interleukin 8, which promotes tissue inflammation[51].

In comparison to other red complex bacteria, *T. forsythia* facilitates the development of periodontal disease using different strategies of virulence, evasion and avoidance of immune detection. One of the strategies is to decorate surface with glycans[52,53]. *T. forsythia* possesses gene that encodes UDP-N-acetyl-D-mannosaminuronic dehydrogenase (*wecC*). This protein is involved in exopolysaccharide biosynthesis. Expression of *wecC* gene increase ability of *T. forsythia* to form biofilm[54].

Biofilm of the Red Complex

The tri-species consortia discussed above is capable of forming biofilm *in vivo* and *in vitro*. The structure and composition of red complex biofilm has not been characterized before and represents the first barrier for periodontal disease attenuation and elimination due to its location at the surface. Carbohydrates of extracellular matrix represent an interest due to ability of maintaining structure, changing morphology of biofilm. Investigation of the gene *sinR* that plays the

regulating role in synthesis of ECM in biofilm of other bacteria, revealed the negative role for exopolysaccharide accumulation[55]. The deletion of the gene resulted in the increased production of exopolysaccharides and changed morphology of the ECM to mesh-like structure, which increased hydrodynamic shear force resistance. The knowledge of carbohydrate composition of biofilm will facilitate in designing the strategy of combating bacterial persistence and antimicrobial resistance due to biofilm formation.

Bacterial Surface Sugars

Bacteria are classified based on the type of cell wall, which can be determined through the Gram-staining technique. Heat-fixed cells are flooded with crystal violet stain followed by addition of Gram's iodine solution (potassium iodide and iodine). The large insoluble in water complex of crystal violet and iodine is formed. Then cells are distained with ethyl alcohol or acetone. During decolorization peptidoglycan layer is dehydrated and tightened. In Gram-positive bacteria during this step large crystals of violet-iodine complex get trapped in peptidoglycan. In Gram-negative bacteria the outer membrane get degraded and thin peptidoglycan layer is not able to retain the crystal violet-iodine complex, therefore, the colour is lost. The counterstain with safranin gives red color to Gram-negative bacteria and does not interfere with purple colour of Gram-positive bacteria[56].

Peptidoglycan of Gram-negative bacteria is found between outer and inner membranes[56]. The outer leaflet of the outer membrane of majority Gram-negative bacteria has lipopolysaccharide, which play important role in virulence[56]. (Figure 1).

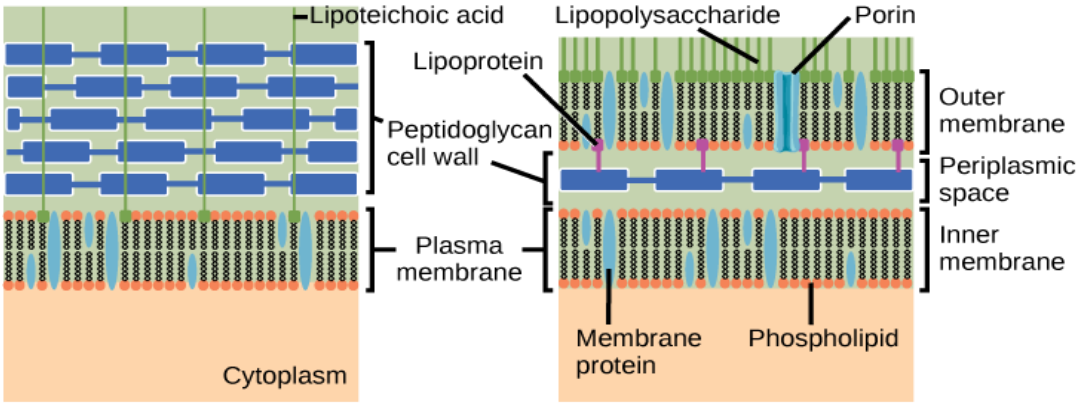

Figure 1: Major differences between two types of cell membranes. The Gram-positive (left) and Gram-negative (right) cell walls. Peptidoglycan is a top thick layer in Gram-positive bacteria, while in Gram-negative it is thin layer located between outer and inner membranes. http://simbac.gatech.edu.- Accessed March 10, 2019

Some bacteria secret and surround itself with polysaccharides named exopolysaccharides (EPS). EPS play important role in protection, survival and recognition of other cells. Exopolysaccharides can be separated into two groups: capsular polysaccharides, which are linked to the cell surface; and extracellular polysaccharides or slime, which are not connected to the cell surface and important for pathogenicity and biofilm formation[57]. This is a highly charged layer that protects bacteria from desiccation, phage infection, phagocytosis, some therapeutics and others[58].

Bacterial exopolysaccharides are synthesised via different pathways. Four different mechanisms of exopolysaccharide biosynthesis are known (Figure 2): (i) Wzx/Wzy- dependent pathway; (ii) ABC transporter-dependent pathway; (iii) synthase-dependent pathway; and (iv) use of a single protein for extracellular

synthesis[59]. The first three mechanisms require precursor molecules and start synthesis from inside of the cell. Last mechanism does not require precursor molecule and monosaccharides are directly added to the growing polymer strand on the outside of the cell (Figure 2).

Capsular Polysaccharides

Capsular polysaccharides are produced by the majority of Gram-positive and negative bacteria as a first defence against environmental challenges[60]. Capsular polysaccharides (CPS) are external structures of bacterial cells that are covalently linked to the cell surface via lipid-A or with an anchored phospholipid. In some cases, CPS do not have membrane anchors[61]. CPS can be divided into two categories based on their structure. Homo- or heteropolymers joined via glycosidic bond[61] and composed of a range of molecules, which can differ in monosaccharide units and their connection. Branching of the polysaccharide chains as well as substitution of organic and inorganic molecules introduces additional complexity to the structure[61]. This diversity of CPS contributes to the ability to evade immune responses. CPS are also called exopolysaccharides and possess high molecular weight.

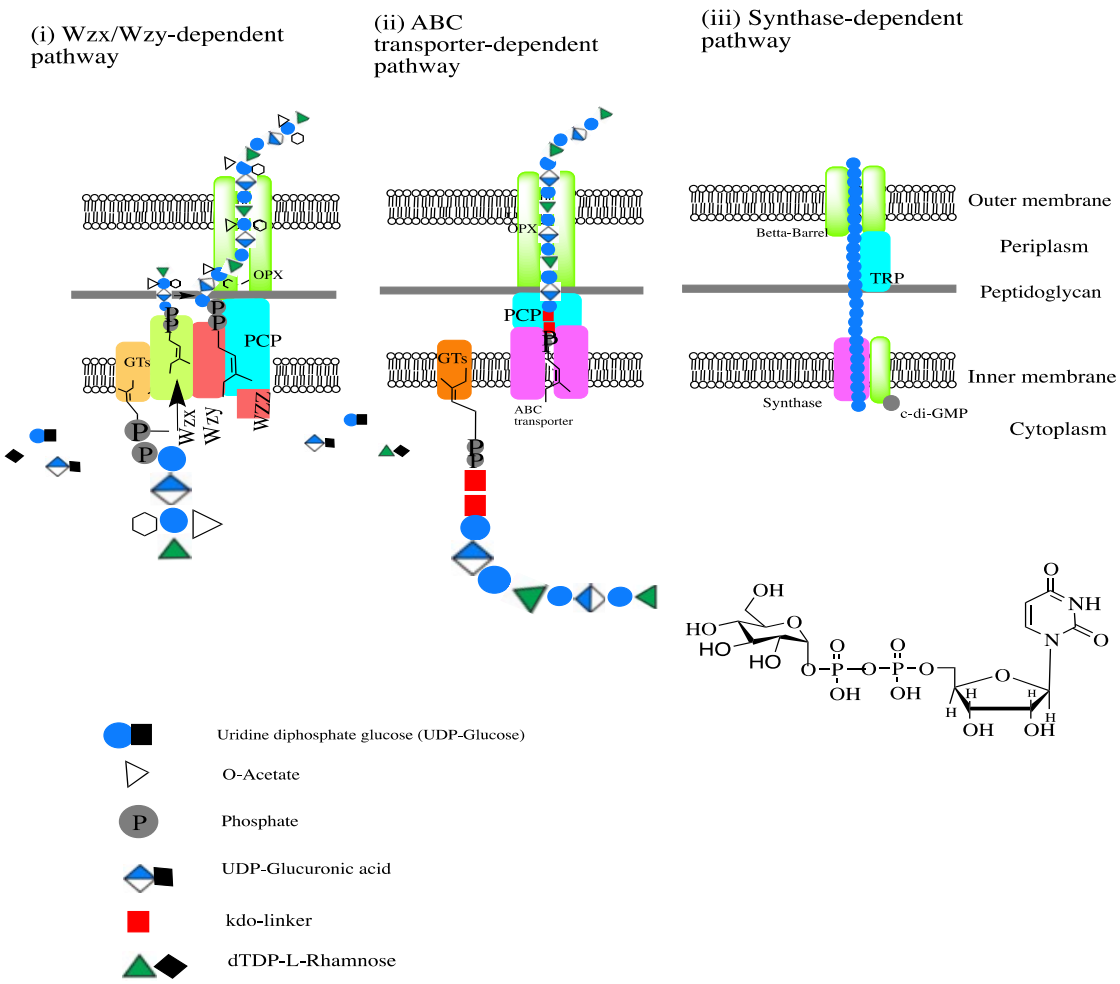

Figure 2: Overview of intracellular EPS biosynthesis pathway. (i) Show the Wzx/Wzy dependent pathway. Repeating units assembled by Glycosyltransferase (GT's) into polymer on the C55-lipid linker. Wzx flippase translocate short polymer into periplasm where Wzy polymerase and co-polymerase protein (PCP) elongate it. PCP and OPX proteins transport polymer across the membrane. (ii) ABC transporter dependent pathway also uses GT's proteins to assemble the polysaccharides, which are anchored on the poly-kdo-linker. PCP and OPX proteins transport polymer across the membrane and cell wall. (iii) The synthase dependent pathway uses synthase complex together with tetratricopeptide repeat (TPR) protein for polymerization and transport of polysaccharide across complete cell envelope[59].

Slime Polysaccharides

Exopolysaccharides secreted to the environment and loosely associated with cell surface are called slime. Slime is distinguished from CPS based the on degree of association with the bacterial surface and the length of the polymer. Some bacteria are capable of producing both types of exopolysaccharides while others only one or the other[60]. The difference between CPS and slime can be complicated due to production of some peripheral material that can be mistaken for slime by cells with excessive production of CPS. There are known cases of mutation of CPS to slimes as well as simultaneous production of both with chemically identical composition[61].

Chemicals to Challenge Biofilm Formation

Formation of the plaque on the surface of the teeth is natural and beneficial to the host. The layer of plaque protects the surface from exogenous harmful bacterial colonization. Bacterial assortment of plaque is stable, despite exposure to different chemical environments. This stability is guaranteed by dynamic balance of microbes. However, this stability can be challenged by regular exposure to low pH due to the consumption of sugar and fermentation of it to lactic acid[13]. In this condition the microflora shifts from Gram-positive to the Gram-negative asaccharolytic anaerobes that are able to thrive in low pH environment. The microbial shift is accompanied by accumulation of plaque around the gingival margin. The build-up in plaque leads to an increased flow of gingival crevicular fluid supplying nutrients to the establish culture. To interfere with breakdown of homeostasis different treatments are used, such as a low concentration of antimicrobial agents, alternative sweeteners and fluoride treatment[27]. These agents

can raise redox potential in the environment and prevent growth and/or metabolism of obligated anaerobes.

There is a dearth of knowledge surrounding the structure and composition of the biofilm produced by red complex. As biofilm production is thought to have a key role in the progression of the periodontal disease, it is of great interest to determine how the structure and composition of the biofilm changes in response to periodontal treatments using different chemicals.

Compound X

In 2006 at the University of Guelph, a new nano-sized phytglycogen material was discovered. The product has a form of glycogen, produced from corn and received a general name that will not be released in this document but will be named compound X. The compound X was tested and showed nutrient value for living cells. Clinical trials show that Compound X helps produce collagen and hyaluronic acid, important for elasticity and hydration of the skin. Previous research results indicate that Compound X have big potential in cosmetic and personal care[62]. The compound is expected to be used in high performance nutrition for athletes and as a drug delivery vehicle in the human body[62]. The possibilities of Compound X are not fully investigated. Multiple Ontario universities received the product in order to discover new applications. Compound X was delivered to the Laurier University in order to investigate its influence in *vitro* on periodontal causing bacteria and biofilm formation[62].

Xylitol

Xylitol is a naturally occurring sugar alcohol in most plants. It has a sweet taste and, therefore, is used as a sugar substitute in some products. Xylitol cannot be metabolised by bacteria to acid as fermentable sugars, and as a result cannot cause tooth decay. Another important feature of xylitol is its ability to inhibit the growth of *Streptococcus mutans*, a primary microorganism responsible for the microfloral shift towards pathogenicity[63]. Bacteria metabolise sucrose to water-insoluble glucans. This process is associated with ability to adhere to the surface. Xylitol at low concentration of 4% decreases production of water-insoluble glucans and other polysaccharides[64].

Fluoride

Low concentrations of sodium fluoride (NaF) are used in oral hygiene and added to water in order to prevent dental caries. This compound blocks enzymes that are responsible for bacterial glycolysis[65] and inhibits carbohydrates utilisation[66]. Fluoride also binds calcium ions from hydroxyapatite, mineral composing the enamel of the tooth surface, and prevents corrosion by acids[67]. Some studies show the concentration of NaF higher than 0.1 μM has negative effect on osteoblasts and, therefore, has inhibiting effect on bone formation[68, 69].

H_2O_2

Hydrogen peroxide (H_2O_2) is usually produced during phagocytic metabolic activity through generation of short-life free radicals. These radicals disturb bacterial cell wall integrity, which may cause cell death[70]. Unfortunately for the host,

P. gingivalis developed protection against hydrogen peroxide damage using iron protoporphyrin IX. Iron protoporphyrin IX is efficient enough to protect from phagocytosis but not higher concentrations of H_2O_2 implemented by host[70]. High concentrations of the compound can cause the damage to the enamel and mouth tissues[71]. The highest concentration that is used in teeth whitening is 30% H_2O_2. The concentration of 0.05% H_2O_2 is efficient enough to be used as prophylactic of periodontitis.

Sage

Salvia officinalis, commonly known as sage, is a woody perennial herb from the mint family. The herb is widely used in culinary for its strong taste and fresh smell. *Salvia* sp. has been used for medicinal purposes by different cultures for a long time against asthma, bronchitis, mouth and throat inflammation and other diseases[72]. Through several studies many beneficial biological activities were established such as anti-inflammatory, antibacterial, antioxidative etc[73]. Native Americans traditionally use *Salvia officinalis* during ceremonies of birth, death or just simply purify mind, body and spirit. Sage is actively used in tea of native people in order to induce sweat and break a fever. Some folk stories say that it is useful to carry small amount in the pocket to protect physical and spiritual aura[74]. Interest in using this plant as an anti-biofilm of Red complex arose from being a part of a smudging ceremony of Native Canadian. Some research has proved the presents and influence on bacterial growth of 1,8-cineole, thujone and camphor [75]. Most of these compounds are terpenoids and found to have antibacterial activity[76].

Tetracycline

Tetracycline is an antibiotic widely used for treatment of bacterial infections, such as cholera, syphilis, acne and others. Tetracycline binds to the small ribosomal subunit 30S of prokaryotes and 40S eukaryotes and blocks the point of entry for charged aminoacyl-tRNA at the A site[77]. This action inhibits protein synthesis but can be reversed if drug is removed. Eukaryotes are insignificantly affected since tetracycline is not actively pumped into their cytoplasm in comparison to prokaryotes. Prokaryotes are able to develop resistance to this drug through efflux pump and transfer the gene encoding the pump through horizontal gene transfer[77].

Carbohydrates in nature

The most abundant monosaccharide in nature is glucose (Glc). In mammals it plays an important role as an energy molecule, as well as a regulator of osmotic pressure of blood[78]. In bodies glucose is transformed into glycogen and precursor of fat for long-term energy storage. Plants synthesize glucose from carbon dioxide (CO_2) and water (H_2O) through photosynthesis[79]. This molecule is also further used for the synthesis of larger biologically important polymers, like starch, cellulose and others[79] (Figure 3).

These two polysaccharides represent the importance of the anomeric orientation on overall structure of the polymer. The anomeric center in cellulose has β-orientation, which allows overall polymer to maintain a linear structure. This feature allows for ideal stacking and, therefore, increased hydrogen bonding between layers giving rigidity to plant cell walls containing this polymer[80]. In contrast, starch possesses α-orientation of the anomeric center, which results in a

staircase-like structure of the polymer. The links between monomers of starch are easily accessible by enzymes and, therefore, makes this polysaccharide ideal for energy storage[81]. Carbohydrates (CH) also serve as signalling molecule, part of DNA and RNA, antibiotics, structural component of mammalian and bacterial cells[78,79,81]. Bacterial polysaccharide secreted to its surroundings as well as on the cell surface play part in adaptation, cell signalling, communication and, therefore, an excellent target for bacteria specific attacks.

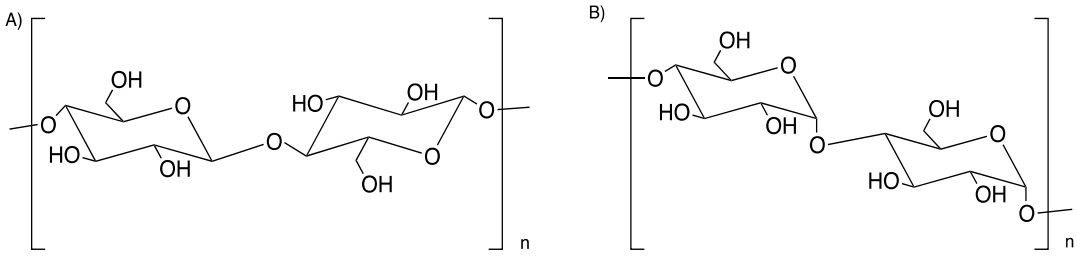

Figure 3: Anomeric orientation of glucose. Units connected in β(1→4) linked D-glucose make up cellulose (A), and units connected in α (1→4) linked D-glucose make up starch (B).

Thesis Statement

Red complex EPS compositional analyses have not been done before. In this study an attempt is made to determine the glycan composition of red complex ECM. The results are compared to the collected data from challenged cultures with NaF, H_2O_2, xylitol, sage, compound X and tetracycline. The goal is to see what sugars are influenced in order to find out if there is a carbohydrate that can be specifically targeted during design of periodontal disease treatment.

The specific aims of the research are: (i) isolate biofilm material formed by red complex and/or individual component species; (ii) identify the components of biofilms, with particular emphasis on glycans; and (iii) compare compositional changes associated with biofilm disruption or maintenance when chemically challenged with commonly used oral treatments.

Methodology

Organisms and Culture Conditions

Treponema denticola ATCC 35405 and *Tannerella forsythia* ATCC 43037 were obtained from the American Type Culture Collection (ATCC, Manassas, VA, USA). *Porphyromonas gingivalis* (pg F0185) was obtained from BEI Resources (Manassas, VA, USA). Organisms were cultured individually and as a mixed culture of all three species (hereafter referred to as "red complex") at 37 °C in Oral Bacterium Growth Medium (OBGM)[48] comprised of the following constituents in (-g/100 ml of milliQ water-): Bacto™ Brain Heart Infusion (Dickinson & Co, MD, USA), 1.25; tryptone powder (BioBasic, Markham, ON), 1.0; yeast extract (BioBasic), 0.75; sodium thioglycolate (BioBasic), 0.05; L-asparagine monohydrate (BioShop, Burlington, ON), 0.025; sodium bicarbonate (Fisher Scientific, NJ, USA), 0.2; D-glucose (BioShop), 0.2; L-ascorbic acid (BioBasic), 0.2; sodium pyruvate (BioBasic), 0.1; sodium chloride (Fisher Chemical), 0.2; ammonium sulfate (Sigma-Aldrich, St. Louis, MO, USA), 0.2; thiamine pyrophosphate (Sigma-Aldrich), 1.2×10^{-4}; menadione (Sigma-Aldrich), 1.0×10^{-4}; haemin (Sigma-Aldrich), 5.0×10^{-5}. Media broth was boiled to dissolve contents, then cooled to room temperature (22 °C) and L-cysteine (Fisher Scientific) 1mg/ml was added. The pH was adjusted to 7.2-7.3 with NaOH and the medium was sterilized. The medium was rapidly cooled to ~40 °C on ice before addition of heat inactivated rabbit serum (Sigma-Aldrich) to a final concentration of 5% v/v, volatile fatty acid mix (0.5% v/v), and *N*-acetylmuramic

acid (0.1 g/L). The solution of fatty acids was prepared in advance, filter sterilized and stored at 22 ^{o}C in the dark. The fatty acid mixture contained 0.1 M potassium hydroxide (Sigma-Aldrich), 0.5% v/v isovolyric acid (Sigma-Aldrich), 0.5% v/v isobutyric acid (Sigma-Aldrich), 0.5% v/v valeric acid (Sigma-Aldrich), 0.5% v/v methylbutyric acid (Sigma-Aldrich). The medium was placed in a Bactron II Anaerobic Chamber (Cambridge Enviromental Products Inc., Kamoka, ON) containing an anaerobic gas mixture of 90% N_2, 5% H_2 and 5% CO_2 for 24 h before inoculation with 1% v/v freezer stock culture. Freezer stock contained 30% v/v glycerol and culture at 0.5 OD_{600}. Each strain was first grown individually to an optical density of 0.2 measured at 600 nm (OD_{600} = 0.2) to ensure early exponential phase growth prior to mixing the three cultures together to generate the tri-species Red Complex culture. Due to different growth rates each strain took different length of time to achieve OD_{600}=0.2: 5 d for *T. forsythia*, 4 d for *T. denticola,* and 2 d for *P. gingivalis*. Before red complex inoculation, *T. forsythia* was diluted 1:5, *T. denticola* was diluted 1:10, while *P. gingivalis* was diluted 1:100 in order to achieve equal cell counts of different culture cells. The media was inoculated to 1% v/v of Red complex mixture. (Christopher Bartlett).

Red complex culture of 10 mL volume was grown in triplicates in Falcon tubes. The culture was collected and subjected to analysis after ECM purification. Wet mass of isolated ECM before lyophilisation was measured using analytical balance. Protein concentration was identified using Bradford assay with Bovine serum albumin (BSA) as a standard. Carbohydrates concentration was measured

using phenol-sulfuric acid assay with mannose as a standard. The average of measures was taken. Standard deviation was calculated.

Challenged Cultures

Red complex 10 ml bacterial cultures were grown in 14 ml falcon tubes in triplicates for each experiment. The cultures were challenged with chemicals widely used in oral hygiene in order to identify crude changes in biofilm composition. The concentrations of added chemicals were identified based on literature and confirmed using previous studies of Sidney Nechacov and Thomas Brenner (members of Drs. Slawson and Weadge labs, respectively). The concentrations were as follows: sodium fluoride (0.01 mg/ml), H_2O_2 (0.05% v/v), xylitol (1 mg/ml), sage extract (5% v/v), compound X and compound Y (1 µg/ml). Tetracycline was used at 0.1 µg/ml final concentration and only for carbohydrates composition and linkage analysis. The chemicals were added at the time of culture inoculation except for the cultures challenged with H_2O_2 and tetracycline. These two cultures were grown for 7 days before addition of chemical to challenge.

Biofilm Collection and ECM isolation

Purification of ECM was performed by modifying a previously described protocol[82] (Figure 4). All centrifugations were done at 4 ^{o}C. Briefly, cells were removed by centrifugation at 5000 × *g* for 30 min and the supernatant was subjected to a second round of centrifugation. Combined cell pellets were collected and stored at -80 ^{o}C for future analysis. Next, the supernatant was mixed with 5 M NaCl to a final concentration of 170 mM and pelleted at 13000 × *g* for 1 h. The

supernatant was collected and stored at -80 °C for future analysis. Pelleted ECM material was washed twice with 10 mM Tris-HCl or 10 mM Na_2HPO_4-HCl buffer pH 7.4. The first wash was subjected to centrifugation for 1 hour at 13 000 × *g*. The second wash was subjected to centrifugation 30 min at 30 000 × *g.* The two supernatants were collected and stored at -80 °C for future analysis. The wet mass of isolated ECM was measured and recorded as the "ECM mass". The ECM pellet was resuspended in the same buffer and subjected to dialysis against MQH_2O for 2 d using a Float-A-Lyzer G2 Dialysis device with a molecular weight cut-off of 100 kDa (Spectrum Laboratories, Inc.). Samples were visualized using SDS-PAGE with stain-free gels (BioBasic) or 14% (w/v) SDS-PAGE gels stained with Coomassie G-250 or silver nitrate.

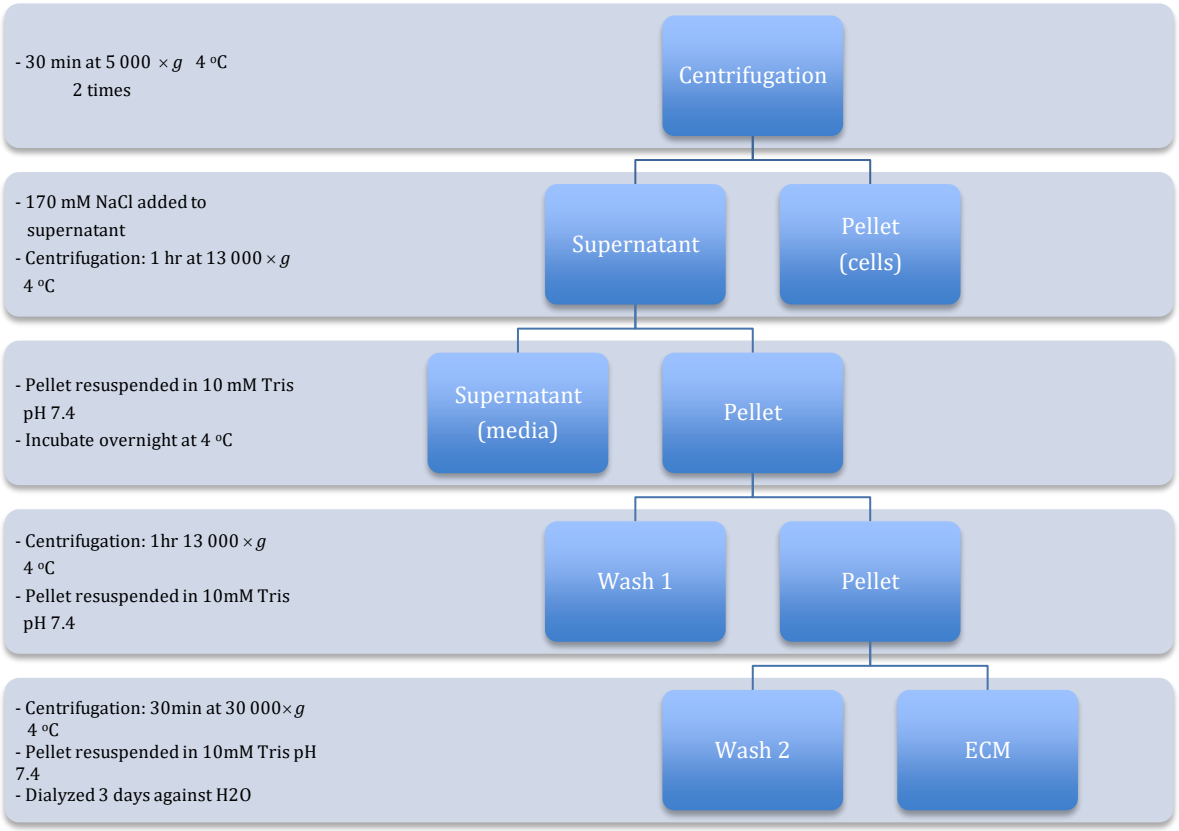

Figure 4: Flow-chart of ECM purification. Culture was subjected to centrifugation to extract ECM. ECM was salt precipitated, followed by two washes. Resulted sample was desalted through dialysis and lyophilized.

ECM Analysis

Protein Concentration

The protein concentration of each isolated ECM was measured using the Bradford assay[83]. Bradford solution contained 0.12 mM Coomassie Blue G-250, 5% (v/v) ethanol, 10% (v/v) of 85% phosphoric acid. Bovine serum albumin was used as a standard. Absorbance of samples was measured at 595 nm and plotted against

the standard curve to determine concentrations.

Protein Visualisation

A Mini-PROTEAN® 3 Cell module (Bio-Rad, Montreal QC) was assembled according to the manufacturers instructions[84]. Sodium dodecyl sulfate (SDS) running buffer consisted of 25 mM Tris-HCl, 1.88% (w/v) glycine, and 10 ml of 10% (w/v) sodium dodecyl sulfate to final 0.1% (w/v). The BioRad stain-free SDS-PAGE gels were made according to the manual[85]. The stacking gel was 4% (v/v), and the resolving gel was 12% (v/v).

An aliquot of 16 µL of each sample was placed in microcentrifuge tubes with 4 µl SDS loading buffer. Sample loading buffer consisted of 62.5 mM Tris-HCl, pH 6.8, 25% (v/v) glycerol, 2% (w/v) SDS, 5% (w/v) beta-mercaptoethanol, and 0.025% (w/v) bromophenol blue. Samples were incubated in a circulating water bath at 95 ^{o}C for 5 min, subsequently cooled down to 22 ^{o}C followed by subjection to centrifugation for 2 min at 14 000 × *g*. Broad range, low range or dual color standard ladder (Bio-Rad) was used in one of the available wells and the gels were subjected to 70 V for 20 min in order to condense and line all sample before entering the resolving part of the gel. For the remaining time, voltage was increased to 120 V, until the bromophenol blue left the gel. Gels were removed from glass plates and visualized using BioRad Gel Doc EZ Imager with a stain-free tray.

Carbohydrate Visualisation

In comparison to protein visualisation where stain-free SDS-PAGE gels were used, SDS-PAGE gels of 14% (v/v) were made for visualization of carbohydrates, as

well as proteins. A resolving gel contained Tris-HCl buffer 0.375 M pH 8.8, SDS 20% (w/v), APS 10% (w/v), TEMED 0.05% (v/v), acrylamide 40% (v/v) /Bis. The stacking gel contained Tris-HCl buffer 0.246 M pH 6.8, acrylamide 30% (w/v), SDS 10% (w/v), APS 10% (w/v), TEMED 0.2% (v/v). The gels were run at 180 V until the bromophenol blue reached the bottom of the gel, approximately 1h.

The visualization of polysaccharides (PS) was done using silver staining according to established protocol[86]. Fixation, staining, and development of PS were done at 22 ^{o}C. PS were fixed by placing the gel into a 40% (v/v) ethanol-5% (v/v) acetic acid solution, for a duration of 16-18 h. PS were then oxidized by shaking the gel for 5 min at 40 rpm in a mixture of ethanol, acetic acid, and periodic acid [40% - 5% - 0.7% (v/v), respectively]. The gel was washed three times with 0.5-1 L of MQH_2O per wash with shaking at 40 rpm for 5 min. The gel was stained at 70 rpm by submerging the gel for 10 min into a 145 mL solution containing ammonium hydroxide (0.5% (v/v)), sodium hydroxide (0.02 M) and silver nitrate (20% (w/v)) (Fisher Chemical). The gel was washed three times by shaking at 40 rpm for 10 min each wash. The gel was visualized by placing it into 200 mL formaldehyde developer, containing citric acid 0.025% (w/v) (Fisher Chemical) and formaldehyde 0.1% (v/v) (Sigma-Aldrich). The development of the bands was observed within 2-5 min. The gel was visualized using a BioRad Gel Doc EZ Imager.

Carbohydrate Concentration

The phenol-sulfuric acid assay was used to measure total carbohydrates in a sample using the method of Masuko *et al*[87]. Briefly, the carbohydrates are dehydrated by reaction with concentrated sulfuric acid and produce derivatives

(Figure 5). In the consecutive step of phenol addition, the colour change was observed. Briefly, sulfuric acid 50% (v/v) then phenol 0.5% (w/v) were added to the sample in rapid succession followed by incubation in a circulating water bath at 90 °C for 5 min, then allowed to cool down to ~22 °C for 5 min. The absorbance of the samples was measured at 490 nm and plotted against the mannose standard curve to determine concentrations (See standard curve Appendix Figure A1). D-mannose of different concentrations was treated the same as the samples in order to create a standard curve.

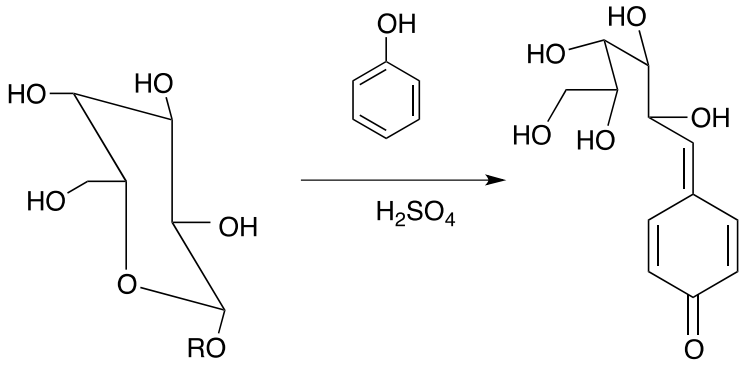

Figure 5: Reaction of saccharide with phenol in acidic condition. The product of the reaction absorbs light at 490 nm and can be used as quantitative measure of carbohydrates.

Carbohydrate Composition Analysis

Sample Preparation

For determination of carbohydrates composition in isolated ECM, samples were subjected to the well-established alditol acetate (AA) procedure[88], in order to

make carbohydrates volatile upon submission to gas chromatography - mass spectrometry (GC-MS). Alditol acetate procedure included 4 steps: hydrolysis, reduction, acetylation, and analysis by GC-MS (Figure 6).

Solid ECM samples of 1.0 mg were added to 1 mL of 4 M trifluoroacetic acid (TFA) (Sigma Aldrich), heated for 4.5 h at 105 ^{o}C, and vortexed every 30 min. Samples were subsequently evaporated at 40 ^{o}C under a gentle stream of compressed air. The resulting monosaccharide mixture of EPS was reduced using sodium borodeuteride ($NaBD_4$) (Sigma Aldrich) in water. This step was crucial to turn aldoses into alditols and keep the open chain structure of a sugar without re-cyclisation. Another beneficial feature of using $NaBD_4$ was that a reduction proceeds at carbon 1 (C-1) position and guarantees distinction between carbon 1 (C-1) and carbon 6 (C-6) position. After addition of $NaBD_4$, samples were left to react for 12 h at 22 ^{o}C on bench. The following steps were done for the removal of tetramethyl borate ($B(OCH_3)_4$) from the solution, which was a by-product of the previous step. A couple of drops of glacial acetic acid (AcOH) (VWR) were added to the reaction to catalyze formation of tetramethyl borate. The mixture was evaporated under 40 ^{o}C and air. The sequential three times addition of methanol (Fisher) and AcOH (95:5) (v/v) mixture and vaporisation to complete dryness aided in removal of $B(OCH_3)_4$.

Acetylation was done at all hydroxyl positions on sugars using 2 mL of concentrated acetic anhydride (Ac_2O) (Sigma Aldrich) and heating to 105 ^{o}C for 90 min, subjecting to vortex every 30 min for even distribution of heat through the sample. This step was followed by evaporation under air and 40 ^{o}C.

The final step in preparation of carbohydrate sample for GC-MS was to remove any basic compounds, water (H_2O) and acetic anhydride (Ac_2O) remaining. For that, the sample was dissolved in dichloromethane (DCM) (Sigma Aldrich), and run through a sodium sulfate (Na_2SO_4) (Fisher) column, packed in a glass Pasteur pipet up to 2 cm high. The eluent was left for 16-18 h to evaporate. The sample in this state can be stored for a long time at 22 ^oC. Before submission to GC-MS the sample was dissolved in 200 µl of DCM.

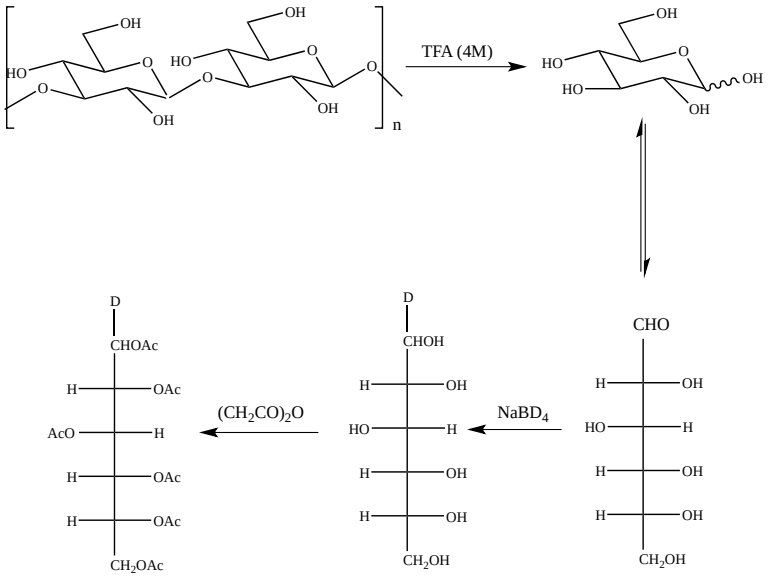

Figure 6: Alditol acetate (AA) analysis method. Scheme of sequential reactions of preparation carbohydrate for GC-MS analysis.

Sample Analysis

The standard monosaccharides were subjected to the same AA procedure and GC-MS chromatograms were saved as a library of carbohydrates. The elution

profiles of alditol acetate prepared samples were compared based on retention times to the standards. Retention times (RT) can slightly vary between the samples. Therefore, the most abundant sugar glucose (Glc) was used as a reference for the relative retention time (RRT) calculations (Equation 1). Retention time of one of the sugars in standard sample was divided by retention time of Glc. The value was used for identification of the retention time of corresponding sugar in comparison to Glc in the sample of interest.

Equation 1

$$RRT = RT\ (unknown\ CH)/\ RT\ (Glc)$$

Peaks in chromatogram not always signify the elution of carbohydrate. Characteristic fragmentation of any sugar can be used as a quick identification of which peak represents monosaccharide elution. Each chromatogram peak was assessed individually based on a mass-spectrometry fragmentation pattern (Figure 7 and 8). A fragmentation pattern of monosaccharides can be predicted and, therefore, characteristic. The ionization results in decomposition through carbon-carbon bond braking creating radical and cation of predicted mass to charge ration (361 m/z, 289 m/z, 217m/z, 145m/z, 73 m/z etc.). The probability of cleavage between acetoxylated backbone carbons is even. Each primary fragment can be further fragmented by loss of acetic acid (-60 m/z) and ketene (-42 m/z). In fragmentation pattern, fragment with 145 m/z ratio usually corresponds to the

elution of saccharide. Therefore, only peaks containing 145 m/z fragment were taken in consideration and relative retention time was calculated.

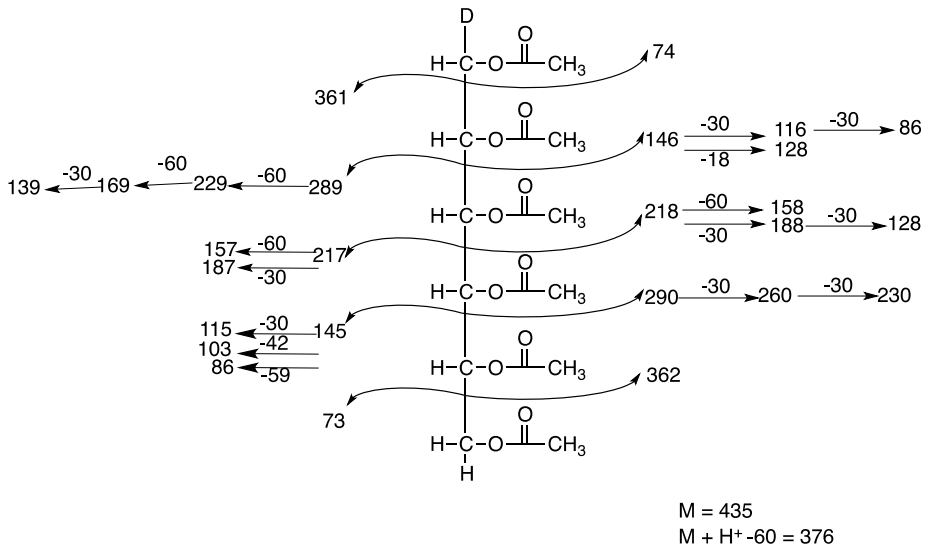

Figure 7: The fragmentation preference of hexose during GC-MS after Alditol Acetate derivatization (AA) shows cleavage between two acetoxylated carbons as primary fragmentation. All hexoses are expected to be fractionated in same pattern and generate same chromatogram peaks unless it has substitution, such as N-acetyl or other. The primary fragment can be further fragmented given expected mass. The characteristic for carbohydrates is fragment mass in 145 m/z

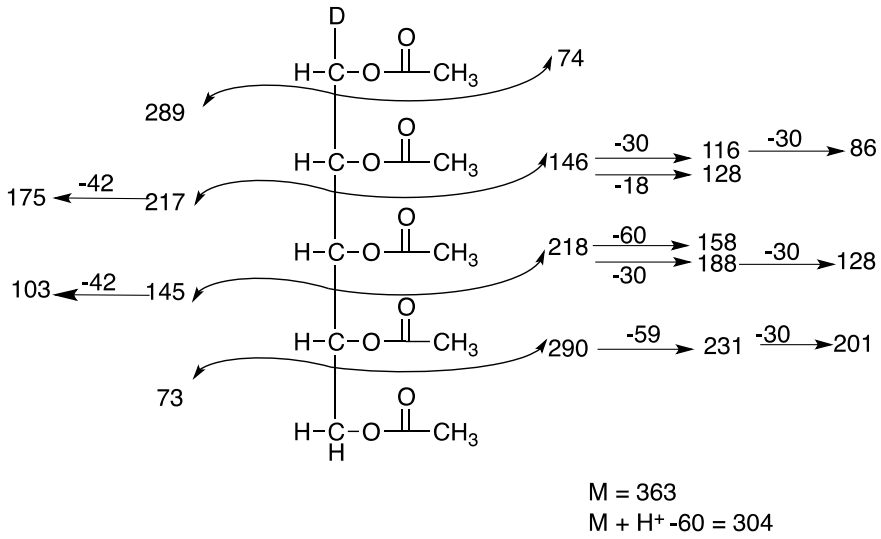

Figure 8: The fragmentation preference of pentose during GC-MS after Alditol Acetate derivatization (AA) shows cleavage between two acetoxylated carbons as primary fragmentation. All pentoses are expected to be fractionated in same pattern and generate same chromatogram peaks unless it has substitution, such as N-acetyl or other. The primary fragment can be further fragmented given expected mass as shown in figure. The characteristic for carbohydrates fragment mass in 145 m/z

Carbohydrate Linkage Analysis

Sample Preparation

For determination of linkage between saccharides in isolated EPS, samples were subjected to the well-established partially methylated alditol acetate procedure (PMAA)[89]. Carbohydrates were derivatized to volatile sugars for gas chromatography-mass spectrometry (GC-MS) analysis. The only difference from AA sample preparation was prior substitution of available hydroxyl groups to methoxy group before hydrolysis. Methylation was followed by alditol acetate derivatization,

where only positions that have been linked to the next carbohydrate would be acetylated or/and have deuteride (Figure 9).

The partially methylated alditol acetate (PMAA) procedure began by dissolving 1.0 mg of sample in dimethyl sulfoxide (DMSO) (Amresco) and stirring for 24 h. In order to generate alkoxide ions, the strong base sodium hydroxide (NaOH) (Amresco) was added to the reaction and mixed for 15 min. Methyl iodide (CH_3I) (Sigma-Aldrich) in a quantity of 2.2 mL was added afterwards for partial methylation of carbohydrate. The solution changed colour to milky-white indicating NaI formation, which is the product of the reaction. The sample was stirred for 4 h. Methylated derivatives were extracted using 3 mL of DCM. Each time the sample was filled with MQH_2O same volume as DCM, shaken vigorously and centrifuged at 2500 × *g*, 10 min. The bottom organic layer was collected. The procedure of addition of water was repeated 3 consecutive times in order to extract partially methylated carbohydrates. The organic layer containing sample in DCM was placed in the new vial and evaporated under air and 40 ^{o}C, followed by alditol acetate procedure.

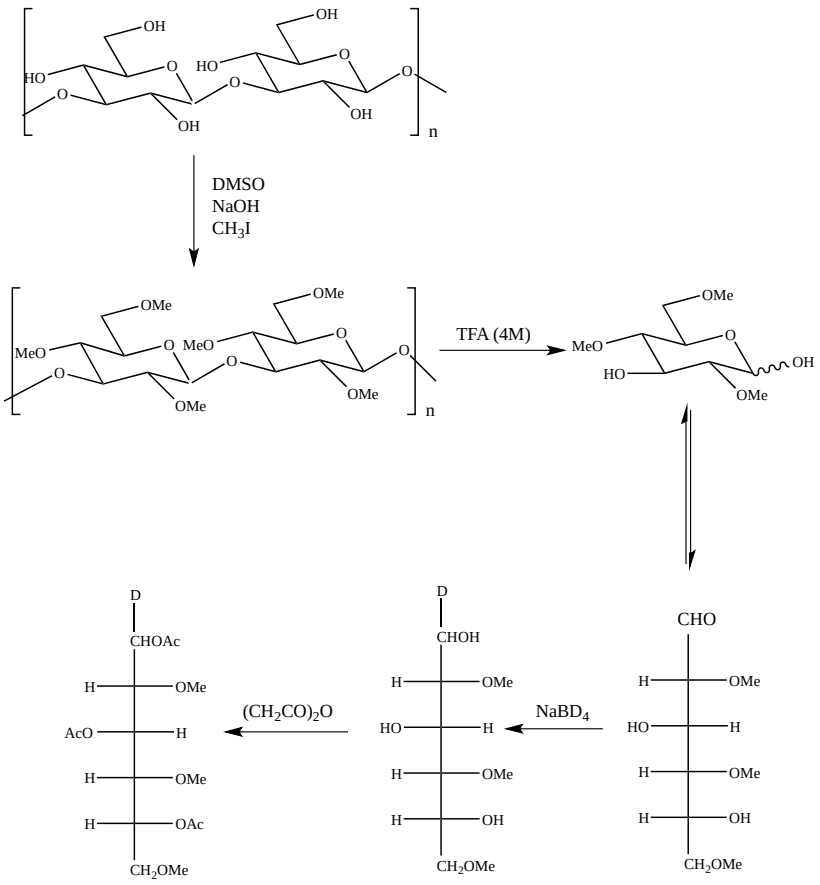

Figure 9: Partially methylated alditol acetate (PMAA) analysis method. Scheme of sequential reactions of preparation carbohydrate for GC-MS analysis.

Partially methylated alditol acetate analysis (PMAA) are used for monosaccharide linkage determination. Similar to AA analysis, retention times of gas-chromatography profile of PMAA samples of EPS can be compared to sugars with known linkage, that have been subjected to (PMAA) prior and saved as a library. The fragmentation pattern of each peak is characteristic to the specific linkage of sugar.

As in AA analysis, the ionization results in radical and cation that is characteristic to primary fragmentation of specific carbohydrate and decomposes through carbon-carbon (C-C) bond breaking. The only difference is that PMAA sugar contains both acetylated and methylated positions, and the probability of splitting C-C bond depends on increased instability of the methoxylated carbons (Figure 10). The secondary fragmentation is possible. For example, monosaccharide can lose acetic acid (-60 m/z), acetoxyl group (-59 m/z), ketene (-42 m/z), formaldehyde (-30 m/z), or methanol (-32 m/z) (Figure 10, 11).

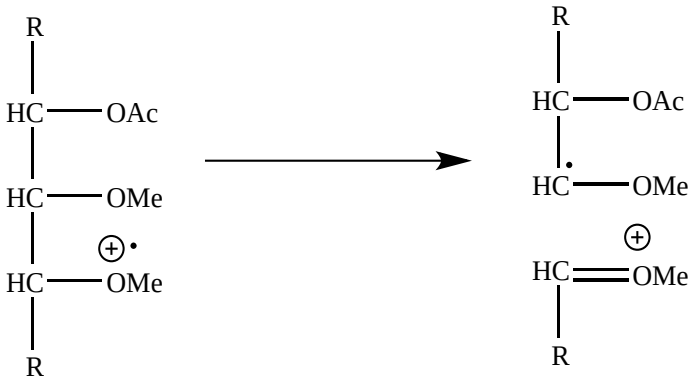

Figure 10: The preference of primary fragmentation for partially methylated sugar (PMAA). Sugar, containing both acetylated and methylated positions, primary splits at unstable methoxylated carbon during GC-MS analysis giving primary cationized fragment and radical with characteristic mass/charge splitting pattern.

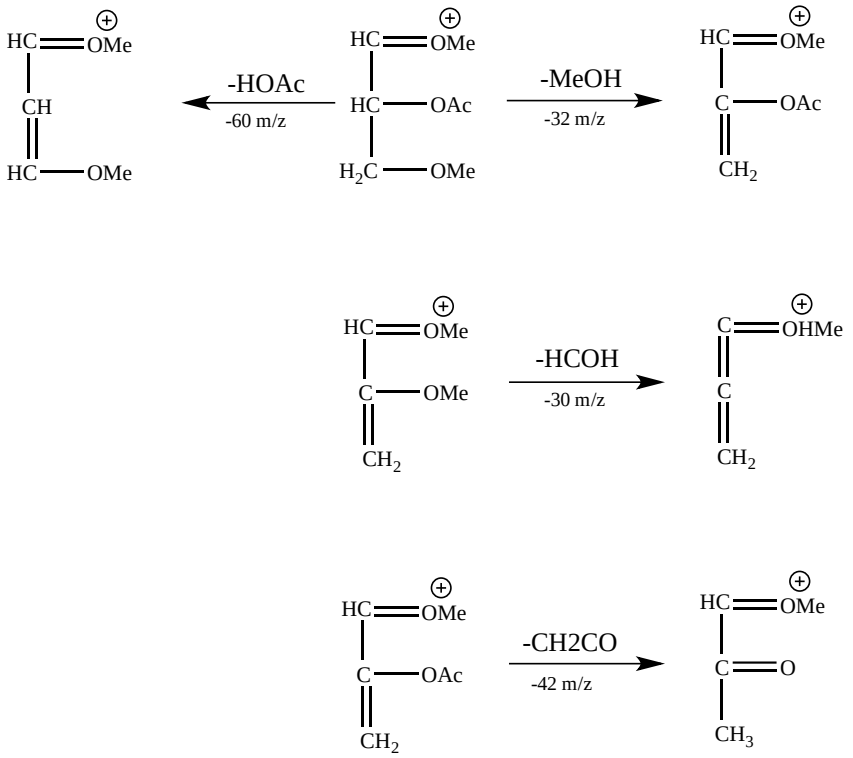

Figure 11: Partially methylated alditol acetate (PMAA) secondary fragmentation pattern. Sugar, containing both acetylated and methylated positions, primary splits at unstable methoxylated carbon during GC-MS analysis giving primary cationized fragments. The cation fragments can be fragmented further losing acetic acid (-60 m/z), acetoxyl group (-59 m/z), ketene (-42 m/z), formaldehyde (-30 m/z), or methanol (-32 m/z).

Gas Chromatography and Mass Spectroscopy

The derivatization of monosaccharides to alditol acetate facilitated the analysis using GC-MS. An Agilent GC-MS contained a HP7890A GC interface with a 5975C mass spectrometer (MS) triple-axis detector set to electron impact (EI) ionization. An Agilent DB5-MS column was used for fragments separation. Column had following parameters: an internal diameter of 30 m x 250 µm, a film thickness of

0.25 µm. The carrier gas helium was used at a flow rate of 1.1 mL/min. The volume of injected sample was 1 µL and used in splitless mode at a 280 °C injection temperature. The equilibration time between each sample was 5 min. The retention times of GC samples were compared to the retention times of standards previously run and these aided in the identification of monosaccharides.

The acquisition mode for MS was in the range of 35.0 – 500.0 amu. The source temperature of MS was 230 °C and the MS quadrupole temperate was 150 °C. Monosaccharides or linkages were identified through examining the fragmentation of daughter ions since data was acquired using a harsh ionization technique (EI mode), where high energy electrons interact with molecule of analyte to produce ions. In order to adequately separate monosaccharides, the oven programs for the AA and PMAA were slightly varied as indicated in Tables 1 and 2 below.

Table 1: GC-MS oven program parameters for AA method

Step	Ramp rate (°C/min)	Final temperature (°C)	Hold (min)
Initial	N/A	37	0.1
1	20	160	20.0
2	20	200	22.3
3	30	250	30.0
4	50	300	1.0
Total sequence run time: 84.2 min			

Table 2: GC-MS oven program parameters for PMAA method.

Step	Ramp rate (°C/min)	Final temperature (°C)	Hold (min)
Initial	N/A	37	0.1
1	20	140	30.0
2	20	180	40.0
3	30	230	30.0
4	50	300	5.0
Total sequence run time: 115.3 min			

Results

Purification

The original isolation of ECM was done in the presence of 25µg/ml Congo red (Sigma Aldrich), which was used in order to facilitate the isolation of ECM from culture as was describe by Lynette Cegelski[82]. The culture of *Pgi* grown with Congo red added to the media had a red color at the time of inoculation and lost its intensity of the colour after 3 d of growth. The control culture without Congo red had consistent colour throughout the experiment and was similar to the final color of the Congo red culture.

Individual cultures were grown for ECM isolation. Four replicates were done in order to determine consistent band patterns. After adjusting purification steps, the consistency of samples images on SDS-PAGE gel of isolated ECM was achieved for each species of bacterial culture (Figure 12). As seen in the figure 12 *Pgi* and red complex consortia produced the most ECM in all three trials. *Tde* and *Tfo* had less mass of isolated ECM and less bands in silver and Coomassie stained gels were observed, indicating of poor production of ECM (Table 3).

The focus of this study is on the red complex ECM. In order to increase replicate, red complex was grown in 10 ml fractions in Falcon tubes. The ECM was isolated and analysed at day zero, one, three, seven and fourteen in order to determine the optimal time for sample collection (Figure 13, 14). Composition of proteins and carbohydrates in red complex culture is shown in Figure 14.

Coomassie stain helped to visualize protein composition, while silver staining helped to visualize proteins and carbohydrates (data in table 3).

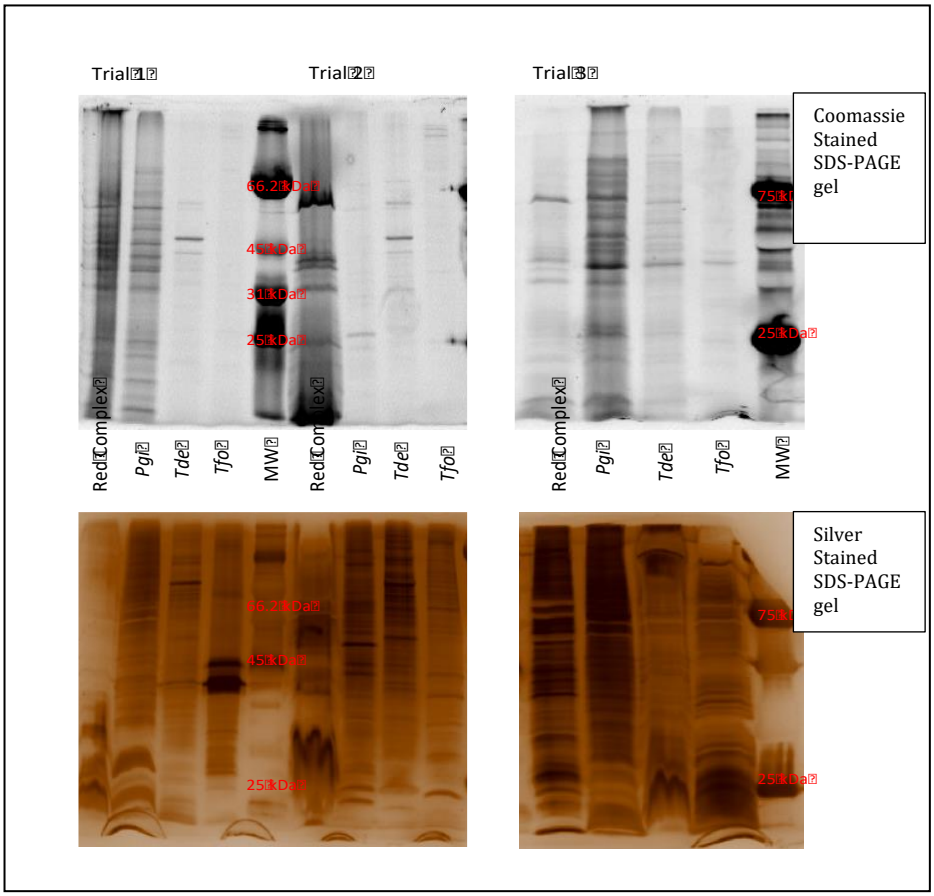

Figure 12: SDS-PAGE visualisation of purified ECM from *Porphyromonas gingivalis, Treponema denticola*, *Tannerella forsythia* and red complex in triplicates. Top gels show different sizes of proteins found in purified ECM. Bottom gels show different sizes of polysaccharides and protein found in purified EPS. From image it is clear that PS predominate over proteins in ECM and *Pgi* is the main biofilm producer in comparison to individual species *Tde* and *Tfo.*

Red complex culture produced the most ECM wet mass (4.79 g) with high concentration of protein (15.7 mg/ml) (Table 3). Individual culture *Tfo* showed the most amount of proteins per mass of isolated ECM in comparison to other cultures (39.13 mg/g of ECM). The mass of isolated ECM was 16 times less in *Tde and Tfo* cultures than in the red complex or *Pgi*. Culture of *Pgi* gave the lease amount of proteins per gram of ECM (3.59 mg/g) within the standard deviation of the red complex culture results (3.59 mg/g).

Table 3: Values measured during EPS purification of Red Complex individual bacteria (*Porphyromonas gingivalis, Treponema denticola*, and *Tannerella forsythia)* and complex growth.

	Volume of culture (ml)	Wet mass of isolated ECM (g)	Bradford assay/ protein concentration (mg/ml)	Protein as proportion mg/g of ECM
Red complex	250	4.79 ± 2.5	15.7 ± 6.8	3.59 ± 1.2
Pgi	250	4.10 ± 2.8	11.2 ± 8.73	3.48 ± 2.09
Tde	250	0.25 ± 0.07	2.45 ± 0.49	10.5 ± 4.9
Tfo	250	0.22 ± 0.2	5.53 ± 4.15	39.13 ± 28.6

In order to establish the best time for ECM collection for the carbohydrate analysis, the red complex biofilm was grown in triplicates and collected at day 3, 7, 14. At the day 3 coomassie stained SDS-PAGE gel show no proteins and silver stained gel show no carbohydrates or proteins in the fractions (Figure 13). At the

day 7, there were some proteins and carbohydrates seen. In comparison to the day 7, samples collected at the day 14 had significant amount of carbohydrates shown by silver-stained SDS-PAGE gel (Figure 13).

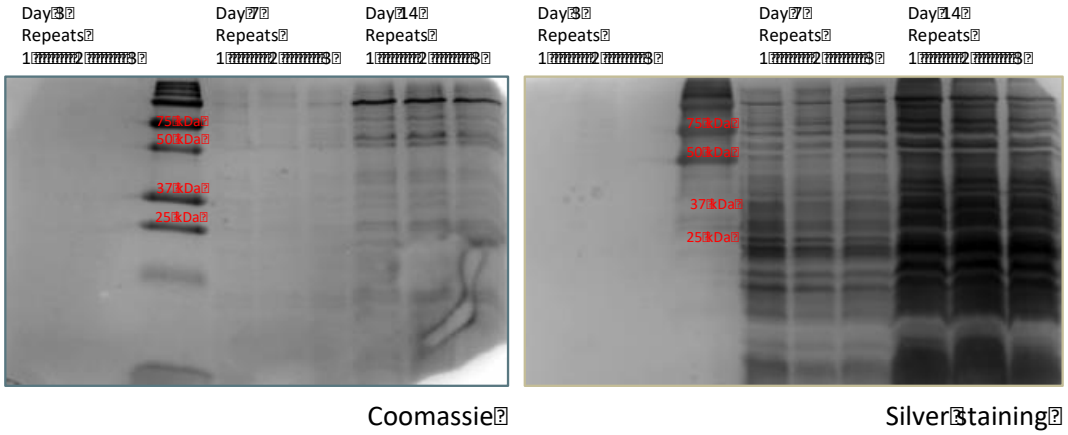

Figure 13: Red complex isolated ECM at day 3, 7, and 14 in triplicates on 14% SDS-PAGE gels stained with coomassie (on left) and silver (on right). Figure shows increase of proteins and carbohydrates compositions in isolated ECM with increased time of growth.

ECM Composition Analysis

Composition analysis of isolated samples were done in triplicates and represented in the Figure 14. The mass of purified ECM increased 3.6 times from 7 d to 14 d, reaching 6.4 mg/ml on the 14 d. Concentration of proteins doubled in same time period reaching to 0.6 mg/ml. Carbohydrates concentration was low at 7 d (0.6 nmol/ml) and increased 26 times by the 14 d (14.6 nmol/ml). The large standard deviation of sugar concentrations could be due to different polysaccharides in the sample and inconsistency of the reaction with phenol during assay. Based on this

information and previous SDS-PAGE visualisation the best time to collect biofilm was day 14.

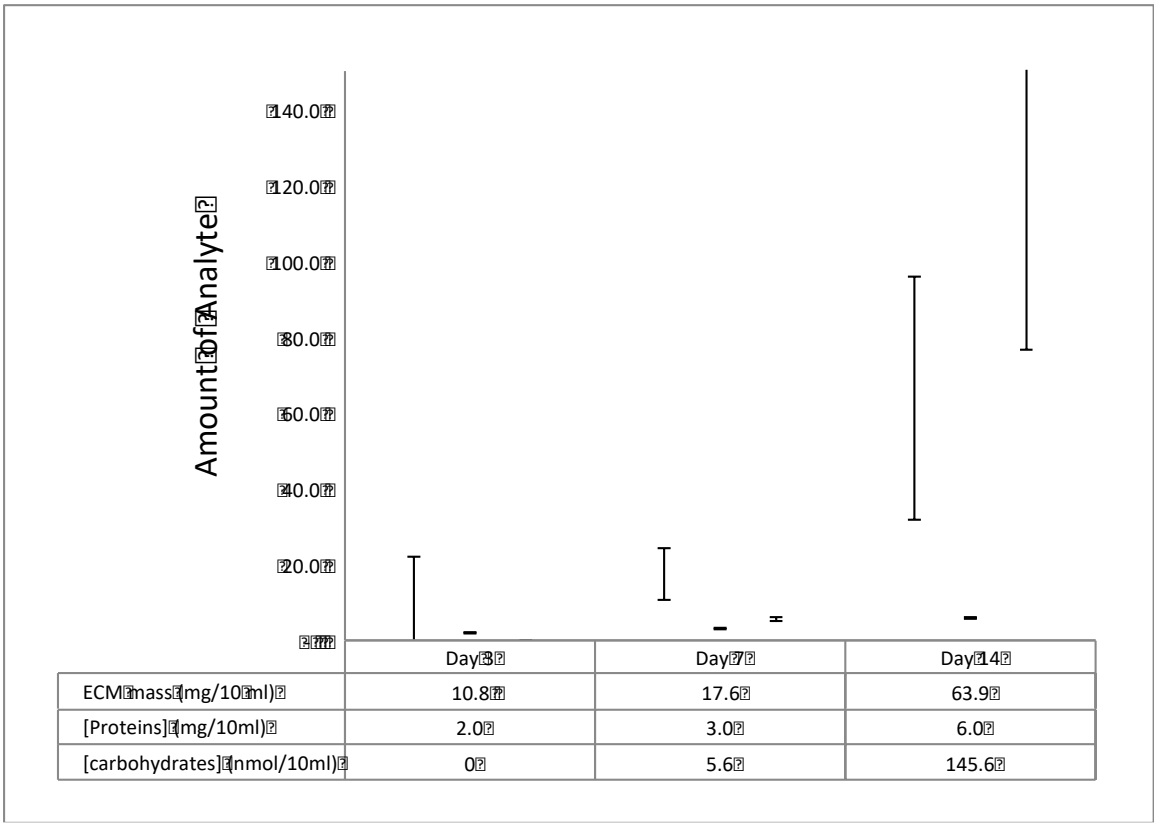

	Day 3	Day 7	Day 14
ECM mass (mg/10ml)	10.8	17.6	63.9
[Proteins] (mg/10ml)	2.0	3.0	6.0
[carbohydrates] (nmol/10ml)	0	5.6	145.6

Figure 14: Analysis of red complex ECM composition at different time of growth. At the day 14, carbohydrates composition increases drastically indicating the maturation of biofilm. The concentration of protein and mass of ECM increased 3 times by the day 14. Protein and carbohydrates concentration were calculated from triplicates of the cultures collected at day 3, 7, and 14. The averaged results are presented with standard deviation.

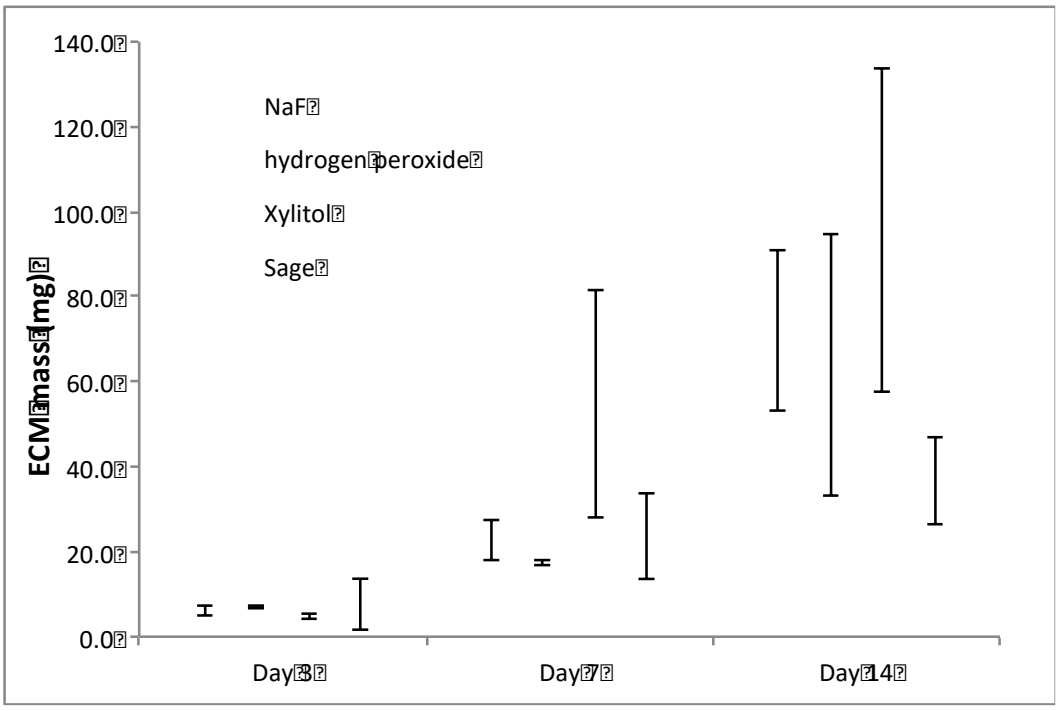

Figure 15: Overtime increase of red complex ECM production in challenged conditions. At the time of inoculation red complex culture was supplemented with sodium fluoride (0.01 mg/ml), xylitol (1 mg/ml), sage extract (5% v/v). Hydrogen peroxide was added on day 7 (0.05% v/v). The volume of the cultures was 10 ml and it was grown in falcon tubes.

The biofilm formation was challenged with different chemicals used in oral treatments. The same concentrations of the chemicals used for oral treatments, was used during this study and showed the ECM production throughout the time line of 14 d (Figure 15). The chemicals were used in order to see the effect of such on crude composition of ECM and carbohydrates composition. For simplicity let's call it "inhibitors". Figure 16 shows all inhibitors used except tetracycline. Tetracycline was used only for the carbohydrate's compositional analysis. Selected chemicals were used in 10 ml falcon tubes cultures in as previously described, and for cultures

grown in Erlenmeyer flask. It was hypothesised that the material of the container for growth would influence the results. Fraction of 10 ml was taken from the flask for analysis.

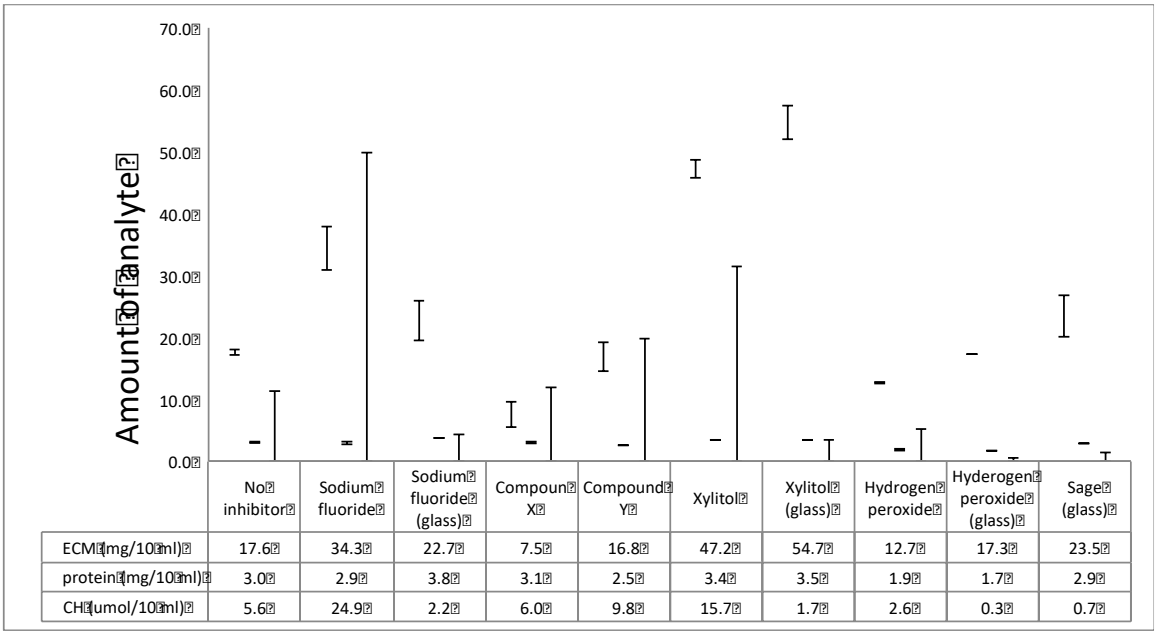

	No inhibitor	Sodium fluoride	Sodium fluoride (glass)	Compoun X	Compound Y	Xylitol	Xylitol (glass)	Hydrogen peroxide	Hyderogen peroxide (glass)	Sage (glass)
ECM (mg/10 ml)	17.6	34.3	22.7	7.5	16.8	47.2	54.7	12.7	17.3	23.5
protein (mg/10 ml)	3.0	2.9	3.8	3.1	2.5	3.4	3.5	1.9	1.7	2.9
CH (umol/10 ml)	5.6	24.9	2.2	6.0	9.8	15.7	1.7	2.6	0.3	0.7

Figure 16: Bar chart of compositional comparison of Red complex ECM challenged at day zero of culture growth. Cultures were inoculated with red complex and grown for 14 days. Inhibitors were added at the day of inoculation except H_2O_2. Hydrogen peroxide was added at the day 7. Volume of the samples was 10ml. Compound X (at 1 mg/mL) significantly decreases amount of EPS produced, while hydrogen peroxide (at 0.05% v/v) and sage extract (at 5% v/v) decreased the concentration of carbohydrates in produced EPS. Cultures grown in Erlenmeyer flasks had less carbohydrates concentration in ECM than same type of cultures grown in falcon tubes.

All samples were collected on the 14 d. The wet mass of isolated ECM grown without inhibitor was 17.6 mg (Figure 16). The mass of ECM grown with NaF was 34.3 mg, which was 1.9 times higher. The culture grown in the glass had less

isolated ECM 22.7mg, which is 1.3 times increase in comparison to uninhibited culture. Although the protein concentration stayed relatively the same 0.30 mg/ml, 0.29 mg/ml and 0.38 mg/ml for uninhibited culture, in falcon tube NaF inhibited and in glass NaF inhibited cultures respectively. The highest concentration of carbohydrates was 2.49 μmol/ml for the NaF inhibited in falcon tube culture, which was 4.4 times higher than uninhibited culture (0.56 μmol/ml) and 11 times higher than NaF inhibited grown in glass.

Compound X and Y were only used in falcon tubes cultures. Compound X showed decrease in the amount of isolated ECM (7.5 mg), which was 2.3 times less than in uninhibited culture (Figure 16). Compound Y was relatively not influential on culture giving almost same amount as uninhibited culture 16.8 mg. The concentration of proteins stayed relatively the same as uninhibited culture 0.31mg/ml and 0.25 mg/ml for compound X and Y inhibited cultures respectively. Carbohydrates concentration in compound X inhibited culture stayed relatively similar to uninhibited culture 0.6 μmol/ml, while compound Y inhibited culture carbohydrates concentration increased 1.75 times (0.98 μmol/ml).

The mass of ECM grown with xylitol was 47.2 mg, which was 2.7 times higher than uninhibited culture (Figure 16). The culture grown in the glass had 54.7 mg of ECM, which is 3.1 times increase and the highest amount isolated among all inhibitors. Although the protein concentration stayed relatively the same 0.30 mg/ml, 0.34 mg/ml and 0.35 mg/ml for uninhibited culture, in falcon tube xylitol inhibited and in Erlenmeyer flask xylitol inhibited cultures respectively. The highest concentration of carbohydrates was 1.57 μmol/ml for the xylitol inhibited in falcon

tube culture, which was 2.8 times higher than uninhibited culture (0.56 µmol/ml) and 9.2 times higher than xylitol inhibited but grown in glass Erlenmeyer flask.

The mass of ECM grown with H_2O_2 was 12.7 mg, which was 1.4 times less than uninhibited culture (Figure 16). The culture grown in the glass vessel had same mass as uninhibited culture 17.3 mg. The protein concentration decreased from 0.30 mg/ml, to 0.19 mg/ml and 0.17 mg/ml for uninhibited culture, in falcon tube H_2O_2 inhibited and in Erlenmeyer flask H_2O_2 inhibited cultures respectively. The concentration of carbohydrates was 2.6 µmol/ml for the H_2O_2 inhibited in falcon tube culture, which was 2.2 times lower than uninhibited culture (0.56 µmol/ml) and 18.7 times less than H_2O_2 inhibited but grown in glass Erlenmeyer flask.

The mass of ECM grown with sage extract was 23.5 mg, which was 1.3 times higher than uninhibited culture (Figure 16). The protein concentration stayed relatively similar to uninhibited culture 0.29 mg/ml. The concentration of carbohydrates decreased by 8 times and was measured 0.7 µmol/ml.

Monosaccharides Composition

Each sample of ECM was subjected to AA analysis. Fragment pattern generated during GC-MS depends on the compound. Some fragment ions (m/z 145, 218) from electron ionization chromatogram (EIC) produced during glycan structural analysis can be useful for selecting peaks corresponding to alditol acetate derivatized carbohydrate[90]. Each peak of GC-MS spectrum of ECM containing 145 m/z fragment was inspected closer. The elution profiles of alditol acetate prepared samples were compared based on retention times to the retention times of

standards used in Dr. Mario A. Monteiro lab (UofG). Negative control was a sample of OBGM media in order to distinguish sugars that come only from ECM. Red complex ECM alditol acetate analysis indicated the presence of Ribose at 20.6 min, mannose (Man) at 31.5 min, glucose (Glc) at 31.8 min, galactose (Gal) at 32.1 min, N-acetylglucosamine (GlcNAc)at 37.5 min, and N-acetylgalactosamine (GalNAc) at 38.9 min (Figure 17). The sample treated with sage indicated the presents of unmatched to the library sugar at retention time of 21.37 min (Figure 18). The samples treated with inhibitors had similar to the red complex untreated with inhibitors profile of sugars. The only difference was in the amount of each sugar detected in the GC-MS analysis chromatogram. Therefore, all samples were done in triplicates and statistical analysis were performed. The hypothesis was made about significant difference between the sets of values. Two-tailed student t-test was used since it is not known which set of values will be bigger/smaller than the other. The data comes from different groups, but the variances are the same (such as temperature, time, nutrients) except one variable "the chemical to challenge biofilm formation". The out-put of excel was probability value (p-values) of student's t-test. The two sets of data considered significantly different if the p-value is less than 0.05. If the value is larger, there are no significant difference observed between sets of data. Statistical analysis revealed no significant difference in the amount of sugars detected in the samples treated with inhibitors in comparison to the sample not treated with inhibitor (See additional information Table A1).

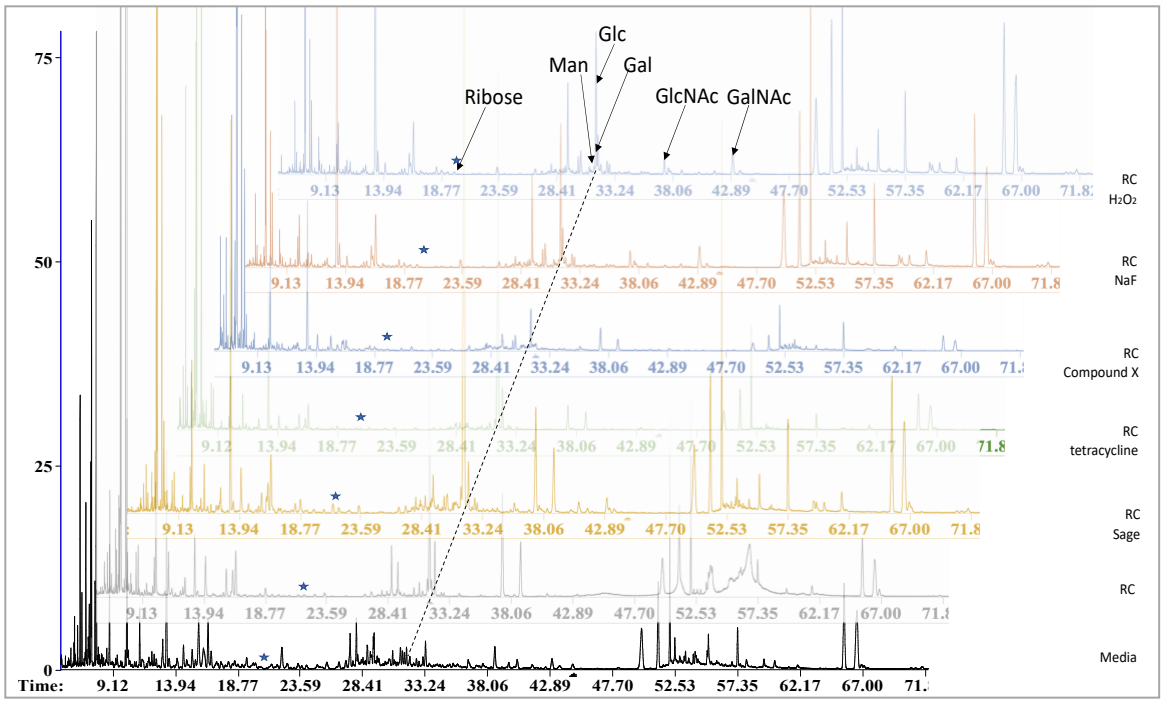

Figure 17: GC-MS chromatogram of sugar composition analysis of red complex ECM from cultures grown with and without challenging chemicals. Samples were collected from 10 ml cultures, purified and 1mg of material was subjected to alditol acetate derivatization. All samples contained ribose, mannose (Man), glucose (Glc), galactose (Gal), N-acetylglucosamine (GlcNAc), and N-acetylgalactosamine (GalNAc).

Glucose is the most easily identified peak in the spectra of carbohydrates and was used to determine linkage. The ion pattern was characteristic to 1,4 – linkage since the 118 and 233 m/z fragments were observed. The linkage analysis of glucose in challenged with inhibitors biofilm revealed no change in comparison to not challenged.

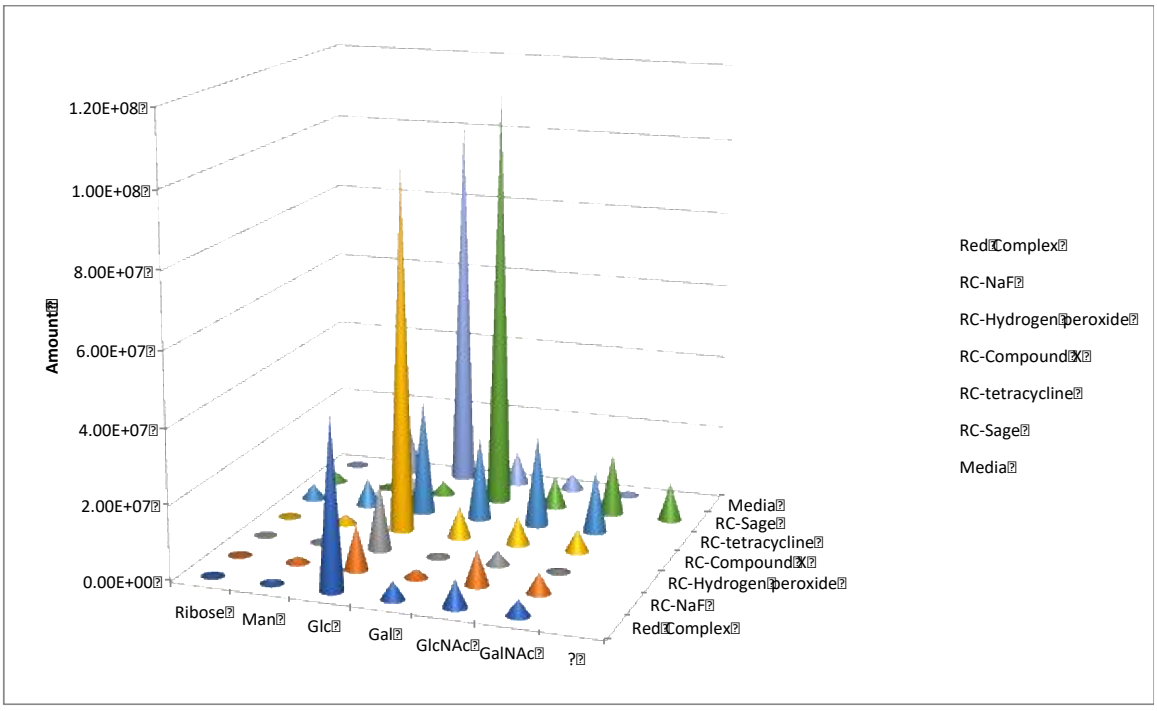

Figure 18: GC-MS detection of different sugars in 1 mg of red complex ECM not inhibited and inhibited by NaF, H_2O_2, tetracycline, sage, compound X. Growth media was analysed as a control sample. Samples were subjected to alditol acetate derivatization prior to GC-MS submission. All samples were done in triplicates. Average area under the elution curve corresponding to the sugar was plotted. (Error bars are not shown).

The red complex ECM together with ECM extracted from biofilm grown in the presence of compound X were given to Dr. Xiaohui Xing (Wade Abbott Group AAFC Lethbridge RDC) for compositional and linkage analysis. Dr. Xing was able to determine sugars in EPS of red complex uninhibited and inhibited with compound X (Figure 19, 20). Independent carbohydrates composition analysis revealed similar results summarized in table 4. Dr. Xing showed the presence of Glc, Man, Gal, GlcNAc, GalNAc in EPS of red complex. The appearance of Ribose in the sample

grown in presence of compound X was observed. Rhamnose sugar was identified by Wade Abbott Group AAFC Lethbridge RDC in both samples.

The elution order of the carbohydrates was similar among studies. The only difference was that Dr. Xiaohui Xing detected Gal before Glc. This could be due to the difference in preparation of the sample to GC-MS as well as method used to separate monosaccharides.

Previous studies suggested the inhibitory influence of ribose on Autoindure 2, which is quorum sensing molecule (QS)[91]. It is possible that bacteria in red complex challenged with compound X may start to produce ribose sugar in order to inhibit quorum sensing and start disassembly of biofilm in order to change location of colonisation. Although, the presence of ribose was detected in this study in the samples not treated with any inhibitors. Statistical analysis did not show significant difference in the amount of ribose in the uninhibited and inhibited cultures.

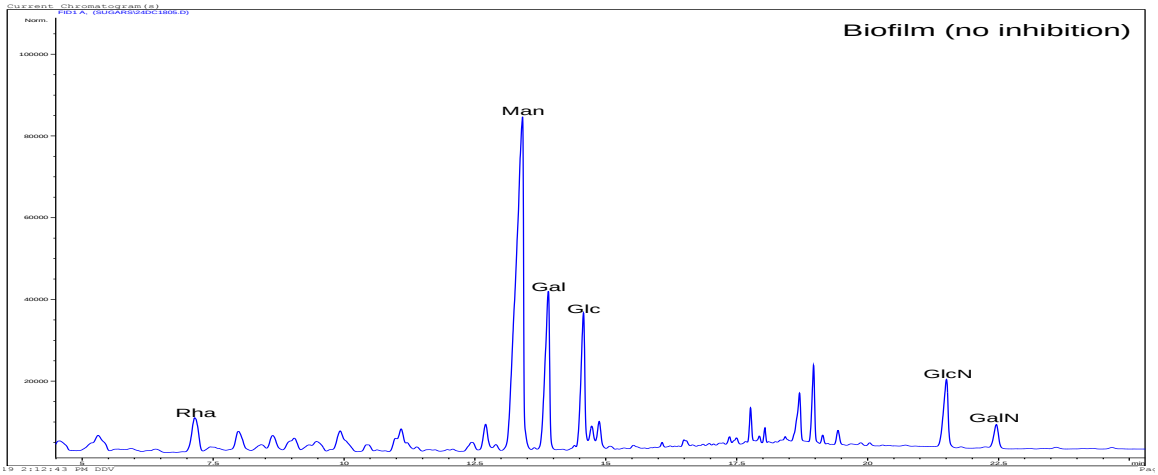

Figure 19: GC-MS chromatogram of Red complex biofilm obtained by Dr. Xing.

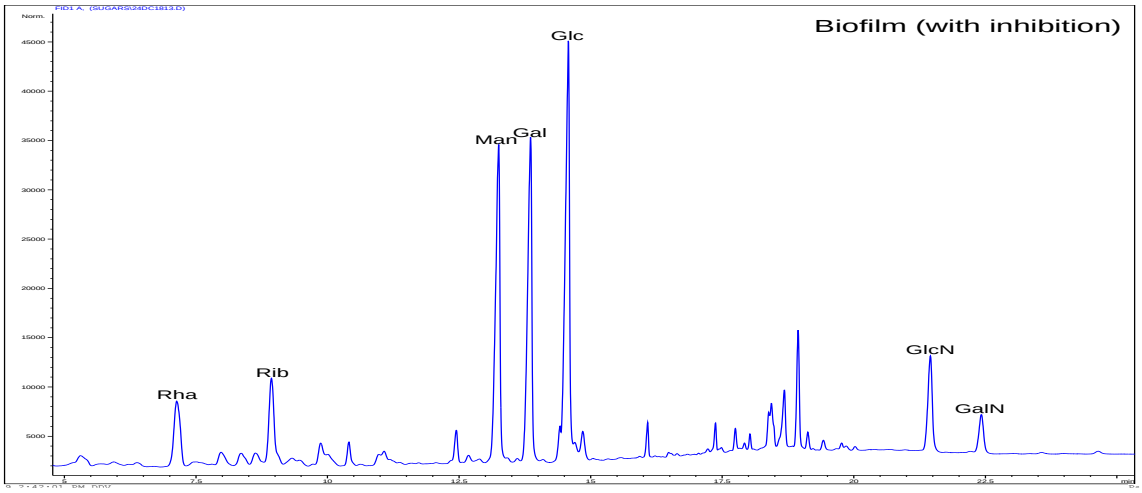

Figure 20: GC-MS chromatogram of Red complex biofilm challenged by compound X obtained by Dr. Xing.

Table 4: Carbohydrates composition of red complex ECM grown with and without compound X. determined by Dr. Xing.

Monosaccharide	Biofilm without inhibition	Biofilm with inhibition
Rha	5.2	6.7
Rib	ND	6
Man	46.5	18.4
Gal	14.1	18.6
Glc	10.3	24.1
GlcN	15.1	15.8
GalN	8.8	10.5

Discussion

During original trials of growth and isolation of red complex ECM 25μg/ml Congo red was used in order to facilitate the ECM isolation. The results of the purification of ECM from the same culture with and without Congo red were similar based on the SDS-PAGE images. The significant influence of Congo red during purification was not observed and, therefore, was not used in further experiments. However, the discoloration of the Congo red in culture could be due to the azo linkage reduction under anaerobic conditions and production of aromatic amines, which are colorless[92].

Cultures containing one member of the red complex were grown and subjected to ECM extraction. Results indicated major production of ECM by *Pgi* (4.1 g per 250 ml culture) since red complex produced 4.79 g per 250 ml culture. Other members of red complex *Tde* and *Tfo* produced 19 times less of ECM (0.25 and 0.22 g per 250 ml culture respectively) (Table 3). The results supported previous studies indicating the insignificant amount of ECM produced by *Tfo*[33] (Figure 12). *Tfo* facilitates the thriving of other members of red complex and as a result biofilm formation by increasing inflammation, decreasing adherence of host periodontal tissue cells and arresting it in G2 phase[53]. Such actions facilitate nutrients supply to red complex.

Silver staining of isolated red complex and individual cultures ECM (Figure 12 and 13) is analyzed in comparison to the Coomassie stained gel of same samples. The increase of the amount of bands in silver stained gels indicated the presence not only proteins but carbohydrates as well.

The increased intensity of the bands in Figure 13 for the 14 d samples in comparison to the 3 or 7 d samples indicates the increased amount of proteins, carbohydrates in isolated ECM. Since the cultures were same volumes 10 ml fractions, the quantitative comparison can be done (Figure 14). At the day 14- increased amount of ECM was isolated which had significant increase of an amount of carbohydrates (26 times). The increased amount of carbohydrates indicates the maturation of biofilm (Figure 14). Since one of the goals of this study was ECM carbohydrates analysis, the best time to collect samples was at 14 day. The cultures challenged with different chemicals also show increase amount of ECM (Figure 15). During analysis of ECM isolated from inhibited cultures was evident that addition of inhibitor does not necessary means decrease of the biofilm formation. Upon addition of 0.01 mg/ml NaF to the culture the amount of isolated ECM increased 1.9 times, where carbohydrates concentration increased in 4.4 times. Bacteria was detecting the threat and was trying to build protective layer biofilm, therefore, the increase in the amount of ECM and carbohydrates concentration is observed (Figure 16). Xylitol supplemented cultures gave similar results, where the ECM amount increased in 2.67 times and concentration of carbohydrates in 2.8 times. Although, the decrease in sugar concentration was observed in cultures grown in glass flasks in comparison to the falcon tubes. This can be explained, that the surface of the container facilitates attachment of the bacteria and, therefore, establishment of the culture and as a result ability to build protective layer biofilm. Compound X (at 1 mg/mL) significantly decreases amount of EPS produced, while hydrogen peroxide (at 0.05% v/v) and sage extract (at 5% v/v) decreased the concentration of

carbohydrates in produced EPS. Cultures grown in Erlenmeyer flasks had significant decrease in carbohydrates concentration in ECM in comparison to same type of cultures grown in falcon tubes based on t-test (results are not shown). According to statistical analysis the change in the amount of ECM or protein concentration was insignificant. These results support idea of importance of carbohydrates in biofilm structure.

All samples were subjected to carbohydrate analysis using GC-MS including samples of the media as a negative control. All samples were done in triplicates. The average results were calculated with standard deviations. According to the GC-MS results every sample including media contained at least 6 sugars in different amounts: ribose, mannose, glucose, galactose, N-acetylglucosamine, and N-acetylgalactosamine (Figure 18). Statistical analysis t-test was performed in order to determine the significance in the amount of specific sugar in the sample. The results indicated that there are no significant difference between amount of specific sugar in the sample inhibited and uninhibited except samples with hydrogen peroxide and samples with tetracycline inhibition. Both samples show significant difference in the amount of mannose and galactose produced (See Table A1). Amount of mannose in tetracycline inhibited sample increased, while in H_2O_2 inhibited sample it decreased. Mannose is important sugar that widely has been found in biofilm of different origin. It plays important roll in maturation and production of the dense biofilm[93]. Therefore, increase production of mannose correlates to increase production of biofilm. Tetracycline is antibiotic that possibly triggers production of protective layer biofilm, therefore significant increase in amount of mannose was observed.

Hydrogen peroxide inhibited cultures, on the other hand, show decrease in amount of mannose. It could be explained that red complex culture could not withstand the given concentration of H_2O_2 (0.05% v/v) and began disassembly of biofilm in order to move away to safer environment.

In case of galactose sugar, similar results were observed. Amount of galactose increased in the tetracycline-inhibited cultures and decreased in H_2O_2 inhibited cultures. Some studies show the galactose toxicity leading to the cell death due to accumulation of galactose metabolic intermediates such as UDP-galactose (UDP-Gal) and phosphorylated galactose (Gal-P) in the absence of essential proteins used in metabolic pathway of galactose[94]. Yunrong Chai *et.al.* showed that UDP-Gal molecule is important in exopolysaccharide biosynthesis, therefore, galactose metabolism plays a main role in formation of biofilm. Whitfield *et.al* studies supported the essences of galactose in production of various exopolysaccharides[94]. The increase of galactose in the sample can indicate the decrease of metabolism of this sugar and therefore, decrease in production of exopolysaccharide in the culture subjected to tetracycline. The mechanism of tetracycline action is inhibition of protein biosynthesis and can possibly be related to the inhibition of the essential for galactose metabolism proteins[95]. The decrease of galactose in the H_2O_2 subjected samples can merely be explained by metabolisms of the sugar.

It would be interesting to test if prolong time (more than 14 days) would have influence on significant change in the amount of saccharides detected by GC-MS.

Conclusion

The specific aims of the research were achieved. During this research, Red complex ECM was successfully grown and isolated. The increase of biofilm wet mass, significant increase of carbohydrates concentrations were observed at the day 14, therefore, established as the best time for biofilm collection and ECM extraction. Further carbohydrate compositional analysis revealed the presence of glucose, mannose, galactose, *N*-acetylglucosamine, and *N*-acetylgalactosamine. Red complex culture was challenged with NaF, H_2O_2, Xylitol, Sage, Cationized nanodendrix, tetracycline. The compositional analysis revealed the increase of mannose and galactose in the sample subjected to tetracycline, while amount of same sugars decreased in the H_2O_2 treated cultures. Other cultures did not show significant change in the amount of saccharides between treated with inhibitors and not treated culture.

Further analysis should be done. Red complex should be grown with and without challenging chemicals past the point of 14 days in order to see if the carbohydrate composition would change.

The results of this study have the potential to identify new mechanisms of biofilm establishment and persistence. These insights may ultimately lead to new methods to disrupt biofilm formation, which could benefit diverse sectors ranging from natural resource extraction, water resource management, and health[96].

Appendix: Additional Information

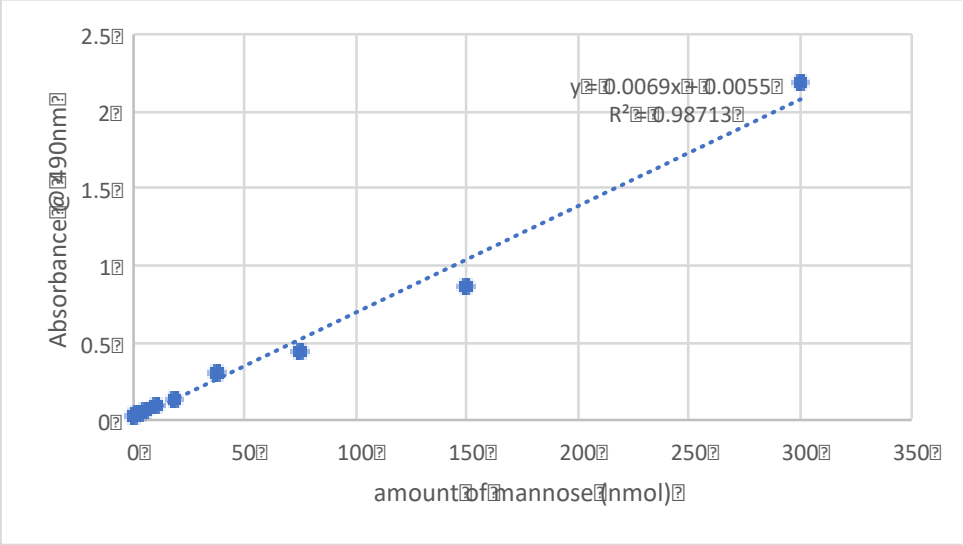

Figure A1: Standard curve for determination of carbohydrates concentration. Different concentrations of Mannose were used in phenol-sulfuric assay. The absorbance of the samples was measured at 490 nm. Constructed standard curve was used for concentration determination of carbohydrates in isolated EPS samples.

Table A1: Raw data collected from GC-MS. Peaks identified the elution of carbohydrates. Are under the peak was used for quantitative estimation of the amount of carbohydrate in the sample. Red complex culture results was compared to the media. Results from the cultures challenged with different chemicals were compared to the red complex culture without inhibition. Statistical t-test p-value equal or less then 0.05 indicates the significant difference between the sample results.

Media	**Area under the peak. Trial 1**	**Area under the peak Trial 2**	**Area under the peak Trial 3**	**Average of areas**	**Standard deviation**	**t-test p-value**
Ribose	1.09E+04	0.00E+00	1.17E+03	4.03E+03	5.99E+03	--
Mannose	3.37E+07	7.26E+05	4.71E+06	1.30E+07	1.80E+07	--
Glucose	2.43E+08	7.85E+05	6.27E+07	1.02E+08	1.26E+08	--
Galactose	2.51E+07	7.53E+05	1.66E+06	9.18E+06	1.38E+07	--
GlcNAc	1.39E+07	3.39E+03	1.99E+03	4.63E+06	8.02E+06	--
GalNAc	4.14E+06	2.52E+03	6.14E+03	1.38E+06	2.39E+06	--
Red Complex (RC)						
Ribose	4.35E+05	0.00E+00	1.65E+04	1.50E+05	2.46E+05	3.62E-01
Man	2.51E+06	5.01E+05	4.72E+05	1.16E+06	1.17E+06	3.17E-01
Glc	5.01E+07	1.40E+07	7.62E+07	4.68E+07	3.12E+07	5.00E-01
Gal	7.14E+06	7.05E+05	7.15E+06	5.00E+06	3.72E+06	6.40E-01
GlcNAc	1.94E+07	7.00E+05	2.47E+06	7.52E+06	1.03E+07	7.21E-01
RC-tetracycline						
Ribose	1.39E+06	1.01E+07	2.02E+06	4.52E+06	4.88E+06	1.97E-01
Man	6.01E+06	1.23E+07	5.50E+06	7.92E+06	3.76E+06	**4.11E-02**
Glc	4.02E+07	3.19E+07	2.20E+07	3.14E+07	9.14E+06	4.57E-01
Gal	1.19E+07	2.82E+07	2.88E+07	2.30E+07	9.60E+06	**3.89E-02**

GlcNAc	9.02E+06	6.12E+07	5.52E+06	2.52E+07	3.12E+07	4.03E-01
GalNAc	4.46E+06	3.36E+07	1.29E+07	1.70E+07	1.50E+07	2.49E-01
RC-H_2O_2						
Ribose	0.00E+00	0.00E+00	0.00E+00	0.00E+00	0.00E+00	1.84E-01
Man	2.13E+06	7.43E+04	2.42E+03	7.36E+05	1.21E+06	**3.46E-02**
Glc	2.90E+07	7.73E+06	1.94E+07	1.87E+07	1.07E+07	1.94E-01
Gal	2.74E+06	2.72E+05	1.43E+05	1.05E+06	1.46E+06	**1.74E-02**
GlcNAc	5.83E+06	1.14E+06	4.00E+06	3.66E+06	2.37E+06	2.98E-01
RC-Compound X						
Ribose	1.47E+06	5.95E+03	0.00E+00	4.91E+05	8.46E+05	3.71E-01
Man	6.28E+06	1.35E+06	1.39E+05	2.59E+06	3.25E+06	4.07E-01
Glc	2.55E+08	3.17E+07	1.22E+07	9.95E+07	1.35E+08	3.59E-01
Gal	2.12E+07	5.01E+06	1.35E+04	8.73E+06	1.11E+07	2.99E-01
GlcNAc	1.89E+07	4.85E+06	4.50E+04	7.92E+06	9.78E+06	5.04E-01
GalNAc	1.52E+07	3.80E+06	1.31E+04	6.32E+06	7.88E+06	2.94E-01
RC-Sage						
	4.10E+06	1.02E+06	3.70E+06	2.94E+06	1.68E+06	n/a
Ribose	0.00E+00	3.12E+03	8.83E+03	3.98E+03	4.48E+03	3.62E-01
Man	8.05E+06	1.33E+06	2.13E+06	3.83E+06	3.67E+06	2.96E-01
Glc	2.68E+08	4.07E+07	3.10E+07	1.13E+08	1.34E+08	4.50E-01
Gal	1.62E+07	2.71E+06	7.53E+06	8.82E+06	6.84E+06	4.43E-01
GlcNAc	4.14E+07	1.06E+07	1.22E+05	1.74E+07	2.15E+07	5.13E-01
GalNAc	2.82E+07	3.01E+06	8.54E+02	1.04E+07	1.55E+07	5.68E-01
RC- NaF						
Ribose	0.00E+00	0.00E+00	1.69E+04	5.64E+03	9.77E+03	8.03E-01
Man	5.33E+06	1.90E+05	4.47E+03	1.84E+06	3.02E+06	5.09E-01

Glc	3.06E+07	7.06E+06	1.28E+03	1.25E+07	1.60E+07	2.66E-01
Gal	6.78E+06	5.95E+05	2.99E+04	2.47E+06	3.74E+06	2.31E-01
GlcNAc	2.73E+07	2.42E+06	6.68E+03	9.91E+06	1.51E+07	6.48E-01
GalNAc	1.56E+07	1.14E+06	4.34E+03	5.57E+06	8.67E+06	6.62E-01

References

(1) Socransky, S. S., Haffaiee, A. D., Cugini, M. A., Smith, C., and Kent, R. L. (1998) Microbial complexes in subgingival plaque. *J Clin Periodontol 25*, 134–144.

(2) Hall-Stoodley, L., Costerton, J. W., and Stoodley, P. (2004) Bacterial biofilms: from the Natural environment to infectious diseases. *Nat. Rev. Microbiol. 2*, 95–108.

(3) Serra, D. O., Richter, A. M., and Hengge, R. (2013) Cellulose as an architectural element in spatially structured escherichia coli biofilms. *J. Bacteriol. 195*, 5540–5554.

(4) Flemming, H.-C., Neu, T. R., and Wozniak, D. J. (2007) The EPS matrix: the "house of biofilm cells". *J. Bacteriol. 189*, 7945–7.

(5) Hans-Curt Flemming, Jost Wingender, Ulrich Szewzyk, Peter Steinberg, S. A. R. and S. K. (2016) Biofilms an emergent form of bacterial life. *Microbiology 14*, 563–575.

(6) Whitfield, G. B., Marmont, L. S., and Howell, P. L. (2015) Enzymatic modifications of exopolysaccharides enhance bacterial persistence. *Front. Microbiol. 6*, 471.

(7) Zaura-Arite, E., Van Marle, J., and Ten Cate, J. M. (2001) Confocal microscopy study of undisturbed and chlorhexidine-treated dental biofilm. *J. Dent. Res. 80*, 1436–1440.

(8) Hollmann, B., Perkins, M., and Walsh, D. (2014) Biofilms and their role in pathogenesis. *J. Microbiol. Exp. 1*, 1–4.

(9) Schooling, S. R., and Beveridge, T. J. (2006) Membrane Vesicles: an Overlooked Component of the Matrices of Biofilms. *J. Bacteriol. 188*, 5945–5957.

(10) Böckelmann, U., Janke, A., Kuhn, R., Neu, T. R., Wecke, J., Lawrence, J. R., and Szewzyk, U. (2006) Bacterial extracellular DNA forming a defined network-like structure. *FEMS Microbiol. Lett. 262*, 31–38.

(11) Lovley, D. R., and Malvankar, N. S. (2015) Seeing is believing: Novel imaging techniques help clarify microbial nanowire structure and function. *Environ. Microbiol. 17*, 2209–2215.

(12) Srivastava, S., and Bhargava, A. (2016) Biofilms and human health. *Biotechnol. Lett. 38*, 1–22.

(13) Houte, J. Van. (1993) Microbiological Predictiors of Caries Risk. *Adv Dent Res 7*, 87–96.

(14) Nozari, A., Rahmati, A., Shamsaei, Z., Hashemi, A. P., Layeghnejad, M.-K., and Zamaheni, S. (2015)

Destructive effects of citric acid, lactic acid and acetic acid on primary enamel microhardness. *J. Dent. Sch. 33*, 66–73.

(15) Singer, S. W., Erickson, B. K., Verberkmoes, N. C., Hwang, M., Shah, M. B., Hettich, R. L., Banfield, J. F., and Thelen, M. P. (2010) Posttranslational modification and sequence variation of redox-active proteins correlate with biofilm life cycle in natural microbial communities. *ISME J. 4*, 1398–1409.

(16) Aas, J. A., Paster, B. J., Stokes, L. N., Olsen, I., and Dewhirst, F. E. (2005) Defining the Normal Bacterial Flora of the Oral Cavity Downloaded from. *J. Clin. Microbiol. 43*, 5721–5732.

(17) Paster, B. J., Boches, S. K., Galvin, J. L., Ericson, R. E., Lau, C. N., Levanos, V. A., Sahasrabudhe, A., and Dewhirst, F. E. (2001) Bacterial Diversity in Human Subgingival Plaque. *J. Bacteriol. 183*, 3770–3783.

(18) Eke, P. I., Dye, B. A., Wei, L., Slade, G. D., Thornton-Evans, G. O., Borgnakke, W. S., Taylor, G. W., Page, R. C., Beck, J. D., and Genco, R. J. (2015) Update on Prevalence of Periodontitis in Adults in the United States: NHANES 2009 to 2012. *J. Periodontol. 86*, 611–622.

(19) Kinane, D. F. (2000) Causation and pathogenesis of periodontal disease. *Periodontology 25*, 8–20.

(20) Beck, J., Garcia, R., Heiss, G., Vokonas, P. S., and Offenbacher, S. (1996) Periodontal Disease and Cardiovascular Disease. *J. Periodontol. 67*, 1123–1137.

(21) Sharma A, Inagaki S, Sigurdson W, K. H. (2005) Synergy between Tannerella forsythia and Fusobacterium nucleatum in biofilm formation. *Oral Microbiol Immunol 20*, 39–42.

(22) Krüger, M., Hansen, T., Kasaj, A., and Moergel, M. (2013) The Correlation between Chronic Periodontitis and Oral Cancer. *Case Rep. Dent. 2013*, 1–8.

(23) Koziel, J., Mydel, P., and Potempa, J. (2014) The link between periodontal disease and rheumatoid arthritis: an updated review. *Curr. Rheumatol. Rep. 16*, 408.

(24) Chandki, R., Banthia, P., and Banthia, R. (2011) Biofilms: A microbial home. *J. Indian Soc. Periodontol. 15*, 111–4.

(25) Hall-Stoodley, L., Costerton, J. W., and Stoodley, P. (2004) Bacterial biofilms: From the natural environment to infectious diseases. *Nat. Rev. Microbiol. 2*, 95–108.

(26) Marsh, P. D. (2005) Dental plaque: Biological significance of a biofilm and community life-style. *J. Clin. Periodontol. 32*, 7–15.

(27) Marsh, P. D. (1994) Microbial Ecology of Dental Plaque and its Significance in Health and Disease. *Adv. Dent. Res. 8*, 263–271.

(28) Socransky S. Sigmund, and Anne, H. D. (2005) Periodontal microbial ecology. *Periodontol. 2000 38*, 1–53.

(29) Tanner, A., Maiden, M. F. J., Macuch, P. J., Murray, L. L., and Kent, R. L. (1998) Microbiota of health, gingivitis, and initial periodontitis. *J. Clin. Periodontol. 25*, 85–98.

(30) Haffajee, A. D., Cugini, M. A., Tanner, A., Pollack, R. P., Smith, C., Kent, R. L., and Socransky, S. S. (1998) Subgingivai microbiota in heaithy, well-maintained elder and periodontitis subjects. *J Clin Periodontoln Periodomoi I99H 25*, 346–353.

(31) Holt, S. C., and Ebersole, J. L. (2005) Porphyromonas gingivalis, Treponema denticola, and Tannerella forsythia: the "red complex", a prototype polybacterial pathogenic consortium in periodontitis. *Periodontol. 2000 38*, 72–122.

(32) Simonson, L. G., McMahon, K. T., Childers, D. W., Morton, H. E., W, C. D., and Baeterial sytiergy, M. H. (1992) Bacterial synergy of Treponetna denticola and Porphyromonas gingivalis in a multinational population. *Otal Microbiol Immunol 7*, 111–112.

(33) Gmur, R., Strub, J. R., and Guggenheim, B. (1989) Prevalence of Bacteroides forsythus and Bacteroides gingivalis in subgingival plaque of prosthodontically treated patients on short recall. *Periodontology 24*, 113–120.

(34) Xie, H. (2015) Biogenesis and function of Porphyromonas gingivalis outer membrane vesicles. *Future Microbiol. 10*, 1517–1527.

(35) Byrne SJ, Dashper SG, Darby IB, Adams GG, Hoffmann B, R. E. (2009) Progression of chronic periodontitis can be predicted by the levels of Porphyromonas gingivalis and Treponema denticola in subgingival plaque. *Oral Microbiol Immunol 24*, 469–477.

(36) Amano, A., Nakagawa, I., Okahashi, N., and Hamada, N. (2004) Variations of Porphyromonas gingivalis fimbriae in relation to microbial pathogenesis. *J. Periodontal Res. 39*, 136–42.

(37) Amano, A., Nakagawa, I., Kataoka, K., Morisaki, I., and Hamada, S. (1999) Distribution of Porphyromonas gingivalis Strains with fimA Genotypes in Periodontitis Patients. *J. Clin. Microbiol. 37*, 1426–1430.

(38) Lo, A., Seers, C., Dashper, S., Butler, C., Walker, G., Walsh, K., Catmull, D., Hoffmann, B., Cleal, S., Lissel, P., Boyce, J., and Reynolds, E. (2010) FimR and FimS: Biofilm Formation and Gene Expression in Porphyromonas gingivalis. *J. Bacteriol. 192*, 1332–1343.

(39) Imamura, T., Banbula, A., Pereira, P. J. B., Travis, J., and Potempa, J. (2001) Activation of Human Prothrombin by Arginine-specific Cysteine Proteinases (Gingipains R) from Porphyromonas gingivalis. *J. Biol. Chem. 276*, 18984–18991.

(40) Takahashi, N. (2015) Oral microbiome metabolism: From "who are they?" to "what are they doing?" *J. Dent. Res. 94*, 1628–1637.

(41) Henry, L. G., McKenzie, R. M., Robles, A., and Fletcher, H. M. (2012) Oxidative stress resistance in Porphyromonas gingivalis. *Future Microbiol. 7*, 497–512.

(42) Liu, Y.-C. G., Lerner, U. H., and Teng, Y.-T. A. (2010) Cytokine responses against periodontal infection: protective and destructive roles. *Periodontol. 2000 52*, 163–206.

(43) Holden, J. A., Attard, T. J., Laughton, K. M., Mansell, A., O'Brien-Simpson, N. M., and Reynolds, E. C. (2014) Porphyromonas gingivalis Lipopolysaccharide Weakly Activates M1 and M2 Polarized Mouse Macrophages but Induces Inflammatory Cytokines. *Infect. Immun. 82*, 4190–4203.

(44) Chu, L., Dong, Z., Xu, X., Cochran, D. L., and Ebersole, J. L. (2002) Role of Glutathione Metabolism of Treponema denticola in Bacterial Growth and Virulence Expression. *Infect. Immun. 70*, 1113–1120.

(45) Yamada, M., Ikegami, A., and Kuramitsu, H. K. (2005) Synergistic biofilm formation by Treponema denticola and Porphyromonas gingivalis. *FEMS Microbiol. Lett. 250*, 271–277.

(46) Grenier, D. (1992) Nutritional interactions between two suspected periodontopathogens, Treponema denticola and Porphyromonas gingivalis. *Infect. Immun. 60*, 5298–301.

(47) Sela, M. N. (2001) Role of Treponema Denticola in Periodontal Diseases. *Crit. Rev. Oral Biol. Med. 12*, 399–413.

(48) Blakemore, R. P., and Canale-Parola, E. (1976) Arginine catabolism by Treponema denticola. *J. Bacteriol. 128*, 616–22.

(49) Limberger, R. J., Slivienski, L. L., Izard, J., and Samsonoff, W. A. (1999) Insertional Inactivation of Treponema denticola tap1 Results in a Nonmotile Mutant with Elongated Flagellar Hooks. *J. Bacteriol.*

(50) Zhu, Y., Dashper, S. G., Chen, Y. Y., Crawford, S., Slakeski, N., and Reynolds, E. C. (2013)

Porphyromonas gingivalis and Treponema denticola Synergistic Polymicrobial Biofilm Development. *PLoS One 8*, 71727.

(51) Posch, G., Pabst, M., Brecker, L., Altmann, F., Messner, P., and Schäffer, C. (2011) Characterization and Scope of S-layer Protein O-Glycosylation in Tannerella forsythia. *J. Biol. Chem. 286*, 38714–38724.

(52) Suzuki, N., Yoneda, M., and Hirofuji, T. (2013) Mixed red-complex bacterial infection in periodontitis. *Int. J. Dent. 2013*, 587279.

(53) Friedrich, V., Gruber, C., Nimeth, I., Pabinger, S., Sekot, G., Posch, G., Altmann, F., Messner, P., Andrukhov, O., and Schäffer, C. (2015) Outer membrane vesicles of Tannerella forsythia: Biogenesis, composition, and virulence. *Mol. Oral Microbiol. 30*, 451–473.

(54) Honma, K., Inagaki, S., Okuda, K., Kuramitsu, H. K., and Sharma, A. (2007) Role of a Tannerella forsythia exopolysaccharide synthesis operon in biofilm development. *Microb. Pathog. 42*, 156–166.

(55) Jessica L. Mark Welch, Blair J. Rossetti,Christopher W. Rieken, Floyd E. Dewhirst, and G. G. B. (2016) Biogeography of human oral Microbiom at the micron scale. *PNAS 113*, E791–E800.

(56) Yamamoto, R., Noiri, Y., Yamaguchi, M., Asahi, Y., and Maezono, H. (2013) The sinR Ortholog PGN_0088 Encodes a Transcriptional Regulator That Inhibits Polysaccharide Synthesis in Porphyromonas gingivalis ATCC 33277 Biofilms. *PLoS One 8*, 56017.

(57) Reckseidler-Zenteno, S. L. (2012) Capsular Polysaccharides Produced by the Bacterial Pathogen Burkholderia pseudomallei. *Intech*. InTech.

(58) Cuthbertson, L., Mainprize, I. L., Naismith, J. H., and Whitfield, C. (2009) Pivotal Roles of the Outer Membrane Polysaccharide Export and Polysaccharide Copolymerase Protein Families in Export of Extracellular Polysaccharides in Gram-Negative Bacteria. *Microbiol. Mol. Biol. Rev. 73*, 155–177.

(59) Schmid, J., Fariña, J., Rehm, B., and Sieber, V. (2016) Editorial: Microbial Exopolysaccharides: From Genes to Applications. *Front. Microbiol. 7*.

(60) Oleksy, M., and Klewicka, E. (2017) Capsular Polysaccharides of Lactobacillus spp.: Theoretical and Practical Aspects of Simple Visualization Methods. *Probiotics Antimicrob. Proteins 9*, 425–434.

(61) Bazaka, K., Crawford, R. J., Nazarenko, E. L., and Ivanova, E. P. (2011) Bacterial extracellular polysaccharides. *Adv. Exp. Med. Biol. 715*, 213–226.

(62) Hamilton, T. (2015) Cornfield of dreams: University of Guelph spinoff Mirexus says its nanosized glycogen particles, isolated in corn, offer a safer and better alternative in a market dogged by controversy. *Can. Chem. News 67*, 34–39.

(63) Söderling, E. M., and Hietala-Lenkkeri, A. M. (2010) Xylitol and erythritol decrease adherence of polysaccharide-producing oral streptococci. *Curr. Microbiol. 60*, 25–29.

(64) Soderling E, Alaraisanen L, Scheinin A, M. K. (1987) Effect of xylitol and sorbitol on polysaccharide production by and adhesive properties of Streptococcus mutans. *Caries Res 21*, 109–116.

(65) Shi, Y., Li, R., White, D. J., and Biesbrock, A. R. (2018) Stannous Fluoride Effects on Gene Expression of Streptococcus mutant and Actinomyces viscous. *Adv. Dent. Res. 29(1)*.

(66) Mandell, R. L. (1983) Sodium Fluoride Susceptibilities of Suspected Periodontopathic Bacteria. *J. Dent. Res. 62*, 706–708.

(67) Subramaniam, P., and Nandan, N. (2011) Effect of xylitol, sodium fluoride and triclosan containing mouth rinse on Streptococcus mutans. *Contemp. Clin. Dent. 2*, 287.

(68) Qu, W., Zhong, D., Wu, P., Wang, J., Han, B., Qu, W.-J., Zhong, D.-B., Wu Jian-Fang Wang, P.-F., and Han, B. (2008) Sodium fluoride modulates caprine osteoblast proliferation and differentiation. *Bone Min. Metab 26*, 328–334.

(69) Lee, H.-J., and Choi, C.-H. (2015) Anti-inflammatory effects of bamboo salt and sodium fluoride in human gingival fibroblasts-An in vitro study. *Kaohsiung J. Med. Sci. 31*, 303–308.

(70) Miller, T. E. (1969) Killing and Lysis of Gram-negative Bacteria Through the Synergistic Effect of Hydrogen Peroxide, Ascorbic Acid, and Lysozyme Downloaded from. *J. Bacteriol. 98*, 949–955.

(71) Eimar, H., Siciliano, R., Abdallah, M. N., Nader, S. A., Amin, W. M., Martinez, P. P., Celemin, A., Cerruti, M., and Tamimi, F. (2012) Hydrogen peroxide whitens teeth by oxidizing the organic structure. *J. Dent. 40*, e25–e33.

(72) Baricevic, D., Sosa, S., Della Loggia, R., Tubaro, A., Simonovska, B., Krasna, A., and Zupancic, A. (2001) Topical anti-inflammatory activity of Salvia officinalis L. leaves: the relevance of ursolic acid. *J. Ethnopharmacol. 75*, 125–132.

(73) Bouajaj, S., Benyamna, A., Bouamama, H., Romane, A., Falconieri, D., Piras, A., and Marongiu, B.

(2013) Antibacterial, allelopathic and antioxidant activities of essential oil of Salvia officinalis L. growing wild in the Atlas Mountains of Morocco. *Nat. Prod. Res. 27*, 1673–1676.

(74) Müller-Ebeling, C., Rätsch, C., and Storl, W.-D. (2003) Witchcraft medicine : healing arts, shamanic practices, and forbidden plants. Inner Traditions.

(75) Jalsenjak, V., Peljnjak, S., and Kustrak, D. (1987) Microcapsules of sage oil: essential oils content and antimicrobial activity. *Pharmazie 42*, 419–20.

(76) Griffin, S. G., Wyllie, S. G., Markham, J. L., and Leach, D. N. (1999) The role of structure and molecular properties of terpenoids in determining their antimicrobial activity. *Flavour Fragr. J. 14*, 322–332.

(77) Chopra, I., and Roberts, M. (2001) Tetracycline Antibiotics: Mode of Action, Applications, Molecular Biology, and Epidemiology of Bacterial Resistance. *Microbiol. Mol. Biol. Rev. 65*, 232–260.

(78) Robyt, F. J. (1997) Essentials of Carbohydrate Chemistry. Springer New York.

(79) V., S. R. (2001) Carbohydrates The Sweet Molecules of Life. Academic Press.

(80) O'sullvian, A. C. (1997) Cellulose: the structure slowly unravels. *Cellulose 4*, 173–207.

(81) White, D., Drummond, J., and Fuqua, C. (2012) Biochemistry of Prokaryotes 1st ed. New York, NY.

(82) Reichhardt, C., McCrate, O. A., Zhou, X., Lee, J., Thongsomboon, W., and Cegelski, L. (2016) Influence of the amyloid dye Congo red on curli, cellulose, and the extracellular matrix in E. coli during growth and matrix purification. *Anal. Bioanal. Chem. 408*, 7709–7717.

(83) Bradford, M. M. (1976) A Rapid and Sensitive Method for the Quantitation of Microgram Quantities of Protein Utilizing the Principle of Protein-Dye Binding. *Anal. Biochem. 72*, 248–254.

(84) BioRad. Mini-PROTEAN ® 3 Cell Instruction Manual.

(85) Bio-Rad. TGX and TGX Stain-Free FastCast Acrylamide Kit and Starter Kit Instruction Manual.

(86) Tsai, C.-M., Frasch, C. E., Sammons, W., Adams, L. D., and Nishizawa, E. E. (1982) A Sensitive Silver Stain for Detecting Lipopolysaccharides in Polyacrylamide Gels. *Anal. Biochem. 119*, 115–19.

(87) Masuko, T., Minami, A., Iwasaki, N., Majima, T., Nishimura, S. I., and Lee, Y. C. (2005) Carbohydrate analysis by a phenol-sulfuric acid method in microplate format. *Anal. Biochem. 339*, 69–72.

(88) Biermann, C. J., and McGinnis, G. D. (1989) Analysis of carbohydrates by GLC and MS. *CRC Press*.

(89) Ruiz-Matute, A. I., Hernández-Hernández, O., Rodríguez-Sánchez, S., Sanz, M. L., and Martínez-Castro, I. (2010) Derivatization of carbohydrates for GC and GC-MS analyses. *J. Chromatogr. B 879*, 1226–1240.

(90) Anumula, K. R., and Taylor, P. B. (1992) A comprehensive procedure for preparation of partially methylated alditol acetates from glycoprotein carbohydrates. *Anal. Biochem. 203*, 101–108.

(91) Jang, Y. J., Choi, Y. J., Lee, S. H., Jun, H. K., and Choi, B. K. (2013) Autoinducer 2 of Fusobacterium nucleatum as a target molecule to inhibit biofilm formation of periodontopathogens. *Arch. Oral Biol. 58*, 17–27.

(92) Bhattacharya, S., and Das, A. (2011) Mycoremediation of Congo red dye by filamentous fungi. *Brazilian J. Microbiol. 42*, 1526–1536.

(93) Rodrigues, D. F., and Elimelech, M. Role of type 1 fimbriae and mannose in the development of Escherichia coli K12 biofilm: from initial cell adhesion to biofilm formation.

(94) Nordlund, A., and Oliveberg, M. (2006) Folding of Cu/Zn superoxide dismutase suggests structural hotspots for gain of neurotoxic function in ALS: Parallels to precursors in amyloid disease. *Proc. Natl. Acad. Sci. 103*, 10218–10223.

(95) Chai, Y., Beauregard, P. B., Vlamakis, H., Losick, R., Kolter, R., and Greenberg, E. E. P. (2012) Galactose Metabolism Plays a Crucial Role in Biofilm Formation by Bacillus subtilis.

(96) Cegelski, L., Marshall, G. R., Eldridge, G. R., and Hultgren, S. J. (2008) The biology and future prospects of antivirulence therapies. *Nat. Rev. Microbiol. 6*, 17–27.